METHODOLOGY SAMPLE SERIES · 002

Taiwan Strait Site Screening

A reference methodology for multi-site metocean comparison

PFT-MS-002 · v1.0 · MAY 2026 · PUBLIC

PF Tech Services Ltd.
沛風科技服務有限公司

Table of contents

What this sample demonstrates

This is the **second** entry in PF Tech's Methodology Sample Series. It demonstrates the complete workflow of an early-stage metocean desktop study on **a three-site cross-segment comparison along the Taiwan Strait offshore-wind belt**. Six capabilities are covered:

- **Multi-source data integration** — ERA5 single-levels (atmosphere / wind / SST) and CMEMS WAVERYS multiyear reanalysis (waves) are ingested into a single reproducible per-site extraction (Sections 2.1, 9).
- **Wind and wave climatology** — annual and seasonal statistics, percentiles, monthly cycles, multi-panel wind-direction roses across the three sites (Sections 3, 4).
- **Operability threshold analysis** — joint Hs / wind tier framework (sensitive / standard / robust) per site, persistence run-length distribution per tier (Section 5).
- **Cross-segment differential analysis** — the headline Site Screening output: which parameters materially distinguish the three segments and which converge across them, with a per-site IBTrACS typhoon-exposure catalogue (Section 6).
- **Alternative-source cross-validation** — per-site spot checks against CWA WW3 10-yr hindcast (seasonal-cycle consistency) and CWA buoy / WAVERYS-NRT (short-window synoptic) at the two nearest buoys (Section 7).
- **Caveat and uncertainty framing** — consolidated limitations grouped by source-data accuracy, spatial-temporal resolution, catalogue scope, and operability-framework choices (Section 8).

How to use this sample

This is a methodology sample, not a project deliverable. It is intended for prospective customers evaluating PF Tech's **Level 1 metocean desktop study** capability:

- **What this report shows**: the depth, framing, and limitation discipline of a PF Tech Level 1 desktop study, demonstrated as the complete workflow on a three-site cross-segment comparison along the Taiwan Strait offshore-wind belt. The methodology and the report structure are the durable contribution; the specific numbers are illustrative.
- **What it is good for**: early-phase site screening, technology selection, feasibility-stage scoping, and weather-window planning conversations with internal stakeholders.
- **What it is not**: a project-specific engineering input. The selection point is a methodology demonstrator, not a real project location, and the values shown are not site-specific design figures — see the Disclaimer on the following page for the scope and liability boundaries.
- **Commissioning a project version**: contact `contact@pft-s.com.tw` with site coordinates, intended use, and timeline to discuss scope.

Table 1: Document information.

Field	Value
Prepared by	PF Tech Services Ltd. — 沛風科技服務有限公司
Web	https://pft-s.com.tw/
Contact	contact@pft-s.com.tw
Period analysed	2019-01-01 to 2023-12-31 (5 years)
Long-term context	2004-01-01 to 2023-12-31 (20 years, ERA5 monthly)
Sites	Three sites along the Taiwan Strait offshore-wind belt — North 25.00°N / 120.44°E, Middle 24.05°N / 119.80°E, South 23.00°N / 119.57°E. Used for methodology demonstration; PF Tech makes no representation about overlap with any specific operating or planned project.
Document version	v1.0 — May 2026
Distribution	PUBLIC. © 2026 PF Tech Services Ltd. All rights reserved, except that this methodology sample may be redistributed in whole or in part subject to the "Required attribution" conditions overleaf.

This document is a methodology demonstration. It may be redistributed in whole or in part, provided that any redistribution retains:

- the document title and PF Tech Services Ltd. credit;
- the data-source attributions in Section 2.1 and Section 9 (required by CC-BY 4.0, the CMEMS Licence, and 政府資料開放授權條款);
- this Disclaimer.

Disclaimer

This report is prepared by PF Tech Services Ltd. — 沛風科技服務有限公司 — to demonstrate the firm's metocean desktop-study methodology.

This report does not constitute a design basis for any specific wind farm, port facility, or coastal asset. The three selection points (listed in the Document information table on the preceding page) were chosen to exercise the complete cross-segment workflow across the Strait; the coordinates are illustrative. The numbers presented illustrate the analysis the methodology produces, not site-specific engineering values.

- The analysis characterizes the sites to a depth appropriate for early-phase site screening, technology selection, and feasibility-stage scoping.
- Engineering design, insurance underwriting, and project-financing decisions typically draw on additional inputs — formal extreme-value analysis, project-specific in-situ measurement, and design-load computation — which PF Tech delivers through a separately scoped engagement.

- The data sources are freely-available reanalysis and observation products used under each source's published licence (see Section 9 for full attribution).
- The three selection points are along the Taiwan Strait offshore-wind belt, chosen for methodology demonstration only; PF Tech makes no representation about whether any of the points falls within any specific operating or planned project area (offshore-wind, port, coastal-engineering, or otherwise).

PF Tech Services Ltd. and its officers, employees, and agents accept no liability for any decision, action, or omission based on the information in this report. Readers requiring metocean data or analysis for a specific project are invited to contact PF Tech directly for a scoped engagement.

Headline findings

> **Within the 2019–2023 screening window, no single Taiwan Strait site dominates across wind, wave, operability, and typhoon-exposure axes — the three sites form a structured three-way trade-off at the screening level. North leads on mean wind resource and has the lowest typhoon-exposure frequency within this 5-year catalogue; Middle carries the *channel-funnelling* wave-tail signature (a Taiwan-Strait-specific wind-acceleration / direction-concentration regime in the central narrow Strait, see §3.1 and §4.1); South leads across operability tiers and on downtime persistence, and is also swell-leading at the *time-mean energy partition level* (§4.5 — this characterises mean-energy composition, not the extreme or operational-limiting sea state, which remains expected to be wind-sea-driven at design events). Single-event extremes (Hs max, typhoon closest-pass) are sample-window dependent and do not equate to design-load envelopes — see the usage-tiering box in the Executive Summary.**

Six-number snapshot of what the methodology produces across the three sites:

Table 2: Headline-finding metrics. Wave / wind absolute maxima and typhoon-frequency rankings are **event-sampled within the 2019–2023 window** — not climatologically stable.

Metric	Value	Note
Annual mean wind10 (N → M → S)	**8.91 → 8.42 → 6.77 m/s**	Clean N→S gradient; ~2.1 m/s gap N–S at 10 m, ~3.0 m/s at 100 m
Annual mean Hs	**N 1.60 ≈ M 1.59, S 1.35 m**	North and Middle essentially tied at mean (~0.01 m gap); both ~16–17% above South
Hs p99 (N → M → S)	4.33 → **4.66** → 3.68 m	Middle leads at the tail by ~8% over North (channel funnelling); South ~15% below North

Metric	Value	Note
Tier-B operability (Hs $\leq$ 2 m, wind $\leq$ 12 m/s)	N 67% / M 68% / **S 80%**	South ~12 pp ahead of Middle and ~13 pp ahead of North (~48 d/yr more standard-ops time vs North; ~45 d/yr vs Middle); §5.1
Tier-B p90 non-operable episode duration	**S 63 h** vs N 90 h, M 106 h	At South, 90% of individual non-operable episodes resolve within 63 h — ~30 / 40% shorter than at North / Middle (§5.2).
Tropical-cyclone exposure rate (Tropical-Storm-level or greater, within 200 km, 2019–2023)	**N 0.6 / yr** vs M 1.2, S 1.6	Frequencies within this 5-year catalogue; not a long-term climatology. North about half the central-Strait rate; South leads. §6.1

The detail behind these numbers is in the Executive Summary on the following page and in §3 – §7. Methodology limits and the boundaries of what these numbers do and do not support are in the structured §8 (15 items across four subsections). §9 carries the full data-source attribution.

Executive Summary

Positioning of this report. The scientific value of this work lies in demonstrating a reproducible early-stage site-screening workflow — *not* in providing design-grade climatological conclusions or new climatological findings for the Taiwan Strait. Read the numbers below with that frame.

How to read this report's numbers — usage tiering. The same numerical analysis can support different decision frames; this report's numbers do not all carry the same weight:

- **Relatively stable for screening-level comparison**: annual / monthly mean wind10 and Hs, seasonal cycle, broad N $\rightarrow$ M $\rightarrow$ S ranking, Tier-B relative operability fraction, the partition energy-fraction picture in §4.5. These are reproducible across data products and stable enough for screening-level comparison across the 2019–2023 window, though they remain subject to interannual variability.
- **Indicative only**: p99 wind / Hs, absolute maxima within the 2019–2023 catalogue, typhoon-event peak Hs, closest-pass minimum at any single site, and the §7.2 buoy / WAVERYS-NRT 30-day bias / RMSE. These carry meaningful single-event noise or single-window noise and should not be treated as stable across resampling.
- **Not design-level**: formal extreme-value analysis (EVA), return periods, design-load envelopes, gust-based operability tier specifications, motion-sensitive vessel envelope work, and any number cited for insurance / project-finance under-writing. These

require dedicated dataset acquisition and analyses beyond this desktop-study stage — see §8.4 items 13–15 and §7.3.

Three sites along the Taiwan Strait offshore-wind belt — **North** (25.00°N, 120.44°E), **Middle** (24.05°N, 119.80°E), **South** (23.00°N, 119.57°E) — were analysed for cross-segment metocean characteristics over **2019–2023** using **ERA5 single-levels** and **CMEMS WAVERYS multiyear reanalysis**. The three sites are chosen approximately 50 km from the nearest Taiwan main-island west coast point (geodesic; method in §2.2), spanning three latitudes of the offshore-wind belt. The headline finding is that **wind10 ranks N > M > S at the annual mean while annual mean Hs is essentially tied at North and Middle (~1.60 m) — and the Hs tail percentiles invert**: the Middle site leads at p95 (3.78 m) and p99 (4.66 m), about 8% above North despite a marginally lower mean wind, consistent with channel-funnelling at the central Strait — a directionally-concentrated wind regime that produces episodically larger seas. The North site has the highest annual mean wind (8.91 m/s); the South site is clearly the calmest by mean (wind 6.77 m/s; Hs 1.35 m) but shows the highest 5-year Hs absolute maximum (7.65 m, attributed to DOKSURI 2023 at 62 km closest pass on 2023-07-27 — see §4.1 / §6.1) and the highest peak periods Tp — consistent with its position south of Penghu, exposed to long-period swell from the open south. The finding has direct implications for site screening at the Taiwan offshore-wind belt: a single-parameter ranking (wind alone) understates the Middle site's tail-extreme Hs exposure and the South site's swell character.

The finding is methodologically supported by:

- **Wind annual + seasonal**: annual mean wind10 N > M > S (8.91 / 8.42 / 6.77 m/s) at 10 m and 10.67 / 9.98 / 7.68 m/s at 100 m, with the N→S gap widening from ~2.1 m/s at 10 m to ~3.0 m/s at 100 m. Seasonal range ~5 m/s summer to ~12 m/s winter; the cross-segment N–S spread is similar in both seasons (~2 m/s) — the annual mean gradient is winter-dominant (§3.1, §3.2).
- **Wave annual + seasonal**: annual mean Hs essentially tied at N and M (1.60 / 1.59 m) with South at 1.35 m (~16% below); Hs p99 M > N > S (4.66 / 4.33 / 3.68 m) — Middle leads at the tail by ~8% over North (channel funnelling) while the gap to South is ~15%. Winter peak monthly mean Hs ~2.7 m at Middle, ~2.5 m at North, ~2.1 m at South in December; summer minima ~0.7–1.0 m across all three, with South marginally above Middle in midsummer from SW-monsoon swell exposure (§4.1, §4.2).
- **Wave directional + spectral structure** (§4.3, §4.4, §4.5): all three sites have tight total-wave directional alignment with the local wind (Hs-weighted $\Delta\theta$ +1.1° to +2.9°), but the **partition decomposition** (§4.5) tells a sharper story than the total-direction or Tp-tail metrics can: North and Middle are wind-sea dominated (WW partition ~55%, SW1 partition ~30%) with NE-aligned swell that is essentially co-directional with the wind, while **South is swell-leading** (SW1 partition **47.9%** of time-mean energy, exceeding WW at 35.0%) with an Hs-weighted SW1 direction of **138° (SE)** — materially off-axis from the local NNE wind. The §4.4 long-period (Tp $\geq$ 10 s) sample fraction (N 3.5% > S 2.9% > M 2.1%) is a coarser swell indicator and only captures the longest events; the §4.5 partition picture is the cleaner cross-segment differential.
- **Operability** (§5): joint-frame Tier-B operability (Hs $\leq$ 2 m AND wind10 $\leq$ 12 m/s) at South 80.3% versus Middle 67.9% and North 67.2% — South's ~12-percentage-point lead corresponds to ~48 more standard-ops days per year. The N–M ordering inverts at the robust tier (Hs $\leq$ 2.5 m, wind $\leq$ 15 m/s): North 81.0% > Middle 78.7%, reflecting that channel-funnelling at the central Strait pushes the wave tail above 2.5 m more often than at the northern Strait exit. Persistence run-lengths reinforce the headline: South has the shortest median non-operable episode (15 h vs 21 h at North and 27

h at Middle) and the shortest p90 non-operable episode duration (63 h vs 90 / 106 h); Middle's one outlier 2,535-hour continuous calm in mid-2022 is the longest single operable run in the catalogue but does not change the median or p90 picture.

- **Typhoon exposure** (§6.1): 2019–2023 catalogue of nine unique tropical cyclones (TCs) passing within 200 km of any site at a lifetime peak intensity of Tropical Storm (TS, $\geq$ 34 kt) or greater — shortened to "TS+" in this report (IBTrACS v4r01, full-archive extraction without spatial pre-filter; §8.2 item 8 documents the extraction methodology). Per-site exposure: **North 3 storms (0.6 / yr), Middle 6 (1.2 / yr), South 8 (1.6 / yr)**. North's frequency is about half the central-Strait rate, physically consistent with Taiwan main-island as a topographic obstacle for systems approaching the northern Strait; North also records the catalogue's only Cat 5 (CHANTHU 2021 at 189 km, 155 kt lifetime peak). Middle has the largest minimum closest-pass in the 5-yr sample (95 km); no 2019–2023 storm passed closer than 95 km to Middle. South has the highest rate and the closer median pass (81 km vs Middle's 131 km), including KOINU 2023 (Cat 4, 120 kt lifetime peak, 100 km closest pass). South Hs max = 7.65 m on 2023-07-27 18:00 UTC is attributed to DOKSURI 2023 (62 km closest pass at that time).
- **Cross-segment differential summary** (§6.2 / §6.3): the three sites form a structured three-way trade-off. Single-parameter ranking is misleading at the screening level: North picks first on mean wind energy and on lowest typhoon-exposure frequency; Middle on typhoon closest-pass cushion and operable-run upper tail; South leads on the operability axis (all three tiers, downtime persistence, mean Hs). The cross-segment view makes the trade-off explicit rather than embedded in a single number.
- **Alternative-source cross-validation** (§7): the CWA WW3 10-yr hindcast cross-checks the WAVERYS 5-yr seasonal cycle at all three sites with mean-Hs Pearson r = 0.98 / 0.97 / 0.77 (N / M / S) and a consistent +0.25 m systematic offset attributable to non-overlapping decadal windows or WAVERYS / MFWAM moderate-wind bias; the CWA buoy (`0-B0075-002`) vs WAVERYS-NRT 30-day check at the two CWA wave buoys (Hsinchu, Qimei) gives Hs RMSE $\approx$ 0.23-0.25 m and Pearson r $\approx$ 0.85-0.88, supporting WAVERYS-family reliability at North (36 km from Hsinchu) and South (22 km from Qimei). Middle has no buoy closer than 96 km, so §7.2 at Middle reports the buoy/model agreement at the geographically nearest buoy (Qimei, 96 km away) as a supporting check rather than a site-direct measurement — the usefulness of this check depends on how representative Qimei is for Middle, which is reduced by the Penghu Islands sitting between the two.
- **Typhoon framing caveat**: ERA5 wind forcing for compact intense tropical cyclones is well-documented as low (~20–40% in peak intensity; Hodges et al. 2017; Schenkel & Hart 2012). The WAVERYS multiyear reanalysis used here partially mitigates this through altimeter-SWH (and post-2017 Sentinel-1 SAR) assimilation, but altimeter overpasses are sparse at eyewall scales, so typhoon-related Hs values in this report should be treated as **indicative rather than design-level** — they likely under-represent compact intense TC peaks. For absolute-extreme design-load analysis, formal extreme-value analysis using the longer 20-year typhoon catalogue is required and is out of scope of this desktop-study report.

The numbers and graphics in §3 – §6 carry these findings in detail; §7 documents the alternative-source cross-validation results; the structured §8 (15 items across four subsections) sets the methodology boundaries; §9 carries the data-source attribution.

1. Site and scope

Three sites along the Taiwan offshore-wind belt are analysed for cross-segment site-screening comparison:

Table 3: Three sites along the western Taiwan offshore-wind belt selected for cross-segment site-screening comparison. The three points are chosen to be approximately 50 km from the nearest point on Taiwan main-island west coast (geodesic distance; method in §2.2), spanning three latitudes of the offshore-wind belt so the comparison is anchored on a consistent distance-from-shore. The south site is south of the Penghu Islands, in the southern Strait proper, exposed to swell propagation from the open south through the Strait–South-China-Sea boundary.

Segment	Latitude	Longitude	Distance to nearest TW coast point
North	25.00°N	120.44°E	~50 km (offshore Hsinchu / Taoyuan)
Middle	24.05°N	119.80°E	~50 km (offshore Changhua)
South	23.00°N	119.57°E	~50 km (offshore Tainan), south of Penghu

→ See **Figure 1** for the spatial layout.

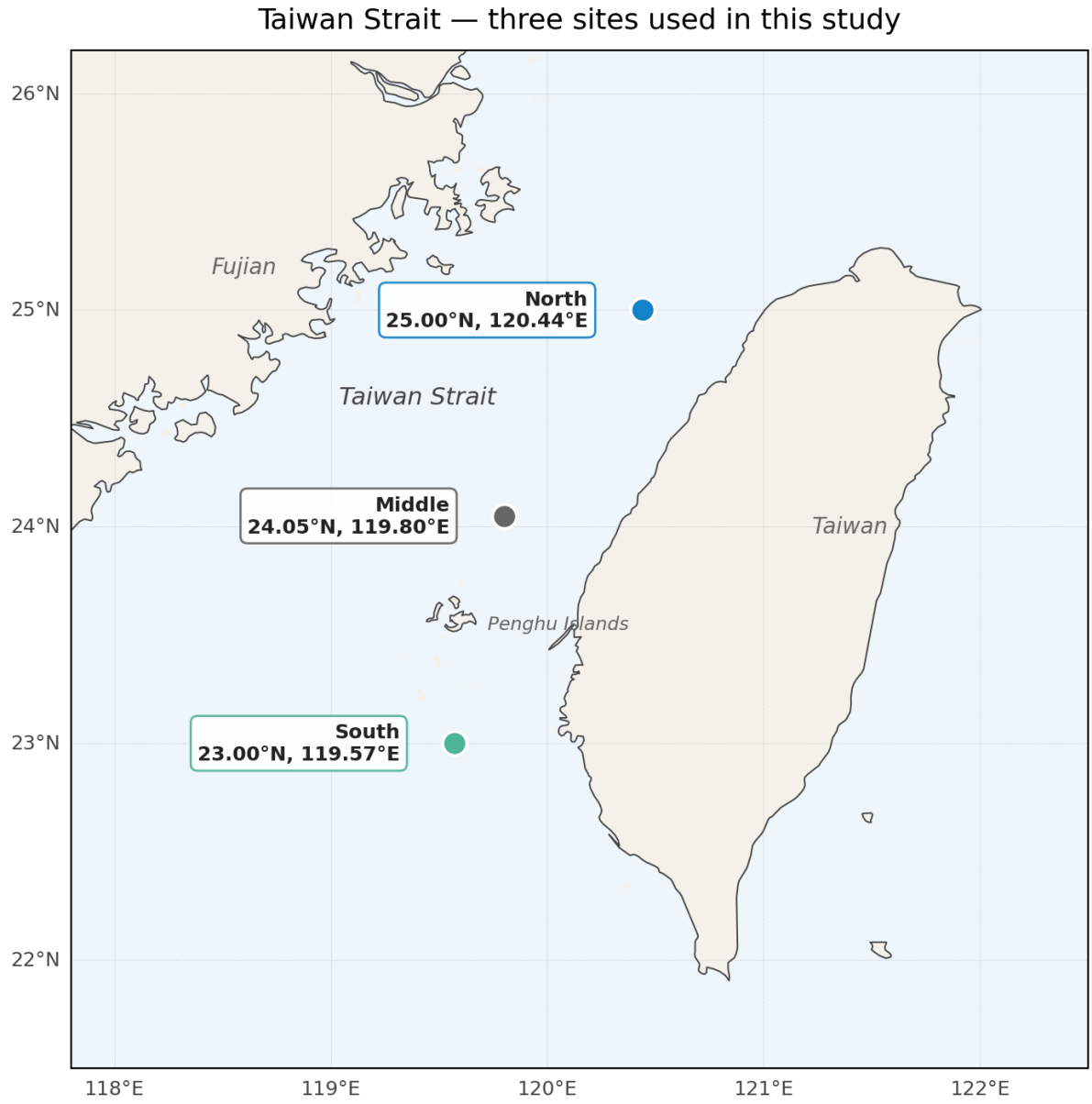

Figure 1: Three Taiwan Strait sites used in this study — North (25.00°N, 120.44°E, blue), Middle (24.05°N, 119.80°E, grey), South (23.00°N, 119.57°E, green). Coastlines from Natural Earth at 10 m resolution. The three points are approximately 50 km from the nearest Taiwan main-island west coast point: North offshore Hsinchu / Taoyuan near the northeast exit of the Strait into the East China Sea; Middle offshore Changhua at the central Strait; South offshore Tainan, south of the Penghu Islands, exposed to swell from the open south.

Reporting framing: three selected points along the Taiwan offshore-wind belt, chosen for methodology demonstration only. The three sites are points on the open-water side of the belt at three latitudes (North, Middle, South); they are **not site-screening recommendations** and should not be interpreted as endorsements of any particular development area. The south site in particular lies south of the Penghu Islands, which is the southern extent of the offshore-wind belt rather than its established core — it is included here as a contrast point for cross-segment comparison, not as a representative development site. PF Tech makes no representation about overlap with any specific operating or planned project. **Equidistant**

offshore principle: each site is approximately 50 km from the nearest Taiwan main-island west coast point (see §2.2 for the distance-to-coast methodology), anchoring the cross-segment comparison on a consistent distance-from-shore. The three coordinates are **methodological anchors for cross-segment comparison**, not lease-area centroids — they do not represent any specific project's representative point, and bathymetric / coastline / Penghu-shadow effects at any particular development would require a site-specific follow-up evaluation. Results are illustrative input to a preliminary desktop-study screening across the three segments.

Spatial context (extraction extent 22–26°N × 117–122°E): The extraction extent encloses all three sites with several grid cells of margin in every direction, providing the spatial neighbourhood for bilinear interpolation at each off-grid coordinate. The extent is intentionally broad enough that all three points are interior to the extracted grid, so the spatial-interpolation methodology is exercised three independent times against the same source grids.

Time scope:

- Main analysis 2019-01-01 to 2023-12-31 (5 years), hourly resolution for wind / atmospheric variables.
- Long-term context 2004-01-01 to 2023-12-31 (20 years), monthly aggregates only.
- Per-site typhoon catalogue (IBTrACS, 2019–2023): §6.1.
- Per-site cross-validation against open observational data (CWA WW3 10-yr climatology + CWA buoy vs WAVERYS-NRT 30-day): §7.

Out of scope (would be addressed in a follow-on engagement): formal extreme-value analysis (EVA, return periods), per-site directional design-load envelopes, numerical-modelling refinement (SWAN / Delft3D / structural response).

---

2. Methodology

2.1 Data sources

Table 4: Data sources used in this study. Full DOIs and dataset version IDs in Section 9. The same 22–26°N × 117–122°E extraction extent covers all three sites.

Source	Variables	Resolution	Period	Licence
ERA5 single-levels (CDS)	u/v 10 m + 100 m, T2m, MSL, dewpoint, SST	0.25°, hourly	2019-2023	CC-BY 4.0
ERA5 monthly aggregates	same 8 variables	0.25°, monthly	2004-2023	CC-BY 4.0
CMEMS WAVERYS reanalysis	VHM0, VTPK, VMDR (+ partition Hs/Tp/dir, Stokes drift)	0.2°, 3-hourly	2019-2023	CMEMS Licence

Full attribution, DOIs, dataset versions, file checksums, and access dates are recorded in the case manifest, available on request.

> **Required attribution — required of any redistribution that includes this section.** This work uses ERA5 reanalysis data (Generated using Copernicus Climate Change Service Information [2026], CC-BY 4.0) and CMEMS WAVERYS multiyear reanalysis (Generated using E.U. Copernicus Marine Service Information; CMEMS Licence). Full citations and DOIs in Section 9.

2.2 Site selection and spatial interpolation

Distance-to-coast. Each site coordinate is chosen so that the geodesic distance (WGS84 ellipsoid) to the nearest point on the Taiwan main-island west coast is approximately 50 km. Coastlines are taken from Natural Earth 1:10m physical land polygons, filtered to the Taiwan main island (a single polygon spanning 21.9–25.3°N). The "sea area" regional anchor (offshore Hsinchu / Changhua / Tainan) for each site is determined by site latitude, independently of the distance-to-coast metric.

Spatial interpolation. Bilinear (canonical) and nearest-neighbour values are both extracted at each of the three sites for every variable. Bilinear is used in all headline numbers; nearest is preserved for sensitivity analysis. The spatial-interpolation methodology is exercised three independent times against the same source grids (ERA5 0.25° × 0.25° and WAVERYS 0.2° × 0.2°), ensuring methodological consistency across the comparison.

Sensitivity of method choice (bilinear vs nearest) on bulk statistics has been verified in prior characterisation work at the middle coordinate (negligible for mean / median / p95; a few-percent shift at absolute extremes). The same regime applies to the north and south sites in this study; explicit per-site sensitivity bars are deferred to a later round.

2.3 Time alignment for joint wind-wave analysis

ERA5 hourly is **down-sampled to the WAVERYS 3-hourly grid** by direct timestamp re-index (00, 03, 06, 09, 12, 15, 18, 21 UTC). WAVERYS is 3-hour instantaneous so this is direct alignment, not temporal averaging. This is the standard and defensible alignment choice — preserves the wave model's native time stamps and avoids fabricating apparent hourly resolution for the wave field.

2.4 Direction conventions

Both wind and wave directions in this report use the **FROM convention** (where the wind / wave is coming from), with 0° = North, clockwise positive — the standard meteorological convention. ERA5 wind FROM-direction is computed from the u/v components; WAVERYS VMDR is verified to use the same FROM convention. The two are therefore directly comparable without any offset, which the directional analyses in §4 rely on.

2.5 Known limitations of source data

This analysis inherits the following known limitations of its source data:

- **ERA5 100 m wind is a model diagnostic**, not an assimilated variable; biases relative to true hub-height wind in stable boundary layers. Project-specific hub-height climatology benefits from validation against a met mast or higher-resolution mesoscale model. The annual-mean shear ratio (100 m / 10 m) at the three sites in this study is ~1.13–1.19, corresponding to a power-law exponent $\alpha \approx 0.05$–0.08 — below the IEC 61400-3 reference $\alpha = 0.14$; this is consistent with ERA5's model-derived vertical structure and should be treated as a known boundary-layer-representation caveat when interpreting hub-height numbers.
- **ERA5 + WAVERYS share atmospheric forcing** (verified). ERA5 wind for compact intense TCs is documented as low (~20–40% in peak intensity; Hodges et al. 2017; Schenkel & Hart 2012); the WAVERYS multiyear reanalysis used here partially mitigates the resulting Hs bias through altimeter SWH (and post-2017 Sentinel-1 SAR) assimilation, but altimeter overpasses are sparse at eyewall scales. Typhoon-period peak Hs at any of the three sites should therefore be treated as **indicative, not design-level**; see §8 for the consolidated limitations statement.
- **ERA5 SST is reanalysis, not satellite observation**; near-coast cells are affected by land contamination. All three sites in this study are far enough offshore ($\geq$ 30 km) to be unaffected, but the same caveat applies to any onshore-shifted variant.
- **ERA5 0.25° smooths the NE-monsoon low-level jet** through the Taiwan Strait; local maxima are slightly understated, in a way that is approximately constant across the three sites and therefore does not bias the cross-segment comparison.
- **WAVERYS 3-hourly vs ERA5 hourly mismatch** is handled by the down-sampling discipline above.
- **5-year analysis window for percentile statistics**: for the hourly ERA5 wind record (43,824 samples per site), the 1% and 5% tails contain ~440 and ~2,200 samples respectively; for the 3-hourly WAVERYS Hs record (14,608 samples per site), the 1% and 5% tails contain ~150 and ~730 samples. Both are stable at annual-mean level but sensitive to the presence or absence of individual typhoon events in the window. A different 5-year window could shift wind p95 by 1–2 m/s and Hs p95 by ~0.5 m at individual sites. Recorded as a caveat to §3.1 and §4.1 percentile numbers.

---

3. Climatology — wind

3.1 Annual statistics — three-site comparison

Percentile note. p95 and p99 are empirical upper-tail percentiles: approximately 5% and 1% of time-series samples exceed these values, respectively. For hourly ERA5 data this corresponds to roughly 18 days/year and 3–4 days/year. They describe upper-tail conditions, not typical conditions; capacity factor depends on the full wind-speed distribution and turbine power curve, not on p95 alone.

Table 5: Three-site annual wind statistics — scalar |U| at 10 m and 100 m above sea level, ERA5 hourly bilinear-interpolated to each site coordinate. n = 43,824 hourly samples per site over 2019–2023 (5 complete years). Wind speed is the scalar mean (|U| computed at hourly resolution then aggregated); vector means would understate climatology and are not used.

Site	n	wind10 mean (m/s)	wind10 p95 (m/s)	wind100 mean (m/s)	wind100 p95 (m/s)
North (25.00°N, 120.44°E)	43,824	8.91	15.82	10.67	18.96
Middle (24.05°N, 119.80°E)	43,824	8.42	16.19	9.98	19.87
South (23.00°N, 119.57°E)	43,824	6.77	13.64	7.68	15.98

The annual mean shows a clean N→S gradient at both heights (10 m: 8.91 → 8.42 → 6.77 m/s; 100 m: 10.67 → 9.98 → 7.68 m/s), consistent with the northeast monsoon strengthening northward along the Strait. The annual gradient is dominated by the winter signal — in summer the three sites converge to within ~1.6 m/s (see §3.2) — so it should not be read as a year-round constant. At 10 m the south site is ~2.1 m/s below the north (8.91 – 6.77 ≈ 2.1 m/s); at 100 m the gap widens to ~3.0 m/s (10.67 – 7.68 ≈ 3.0 m/s). The middle site sits between the north and south at both heights, closer to the north. The p95 ranking differs from the mean ranking — the middle site has the highest p95 at both heights despite a lower mean (p95 16.19 m/s vs north's 15.82 m/s at 10 m), indicating higher tail variance there. The directional component is examined in §3.3, where the middle site shows the tightest concentration in the NNE sector — consistent with a channel-funnelling regime in which a directionally-concentrated, episodically-intense wind drives the p95 above the higher-mean but more directionally-spread north site. The persistence component is deferred to a later round.

3.2 Seasonal cycle — three-site overlay

The seasonal-cycle amplitude is large at all three sites (~6-7 m/s difference between summer minimum and winter maximum) and consistent in phase across the segments — winter maxima driven by the northeast monsoon, summer minima during the southwest monsoon transition. The cross-segment N–S spread is similar in both seasons (~2 m/s in winter at the December peak, ~2 m/s in summer at the August minimum). The middle site tracks the north closely in winter (Dec 12.7 vs 12.4 m/s) and sits between north and south in summer (Aug 5.2 m/s, with N 6.1 and S 4.7). The south site reaches its annual minimum in September (~4.7 m/s), then ramps sharply in October as the NE monsoon onset takes hold; the same Oct ramp is visible at all three sites, with the largest absolute jump at North (Sep 7.2 → Oct 12.0 m/s).

→ See **Figure 2**.

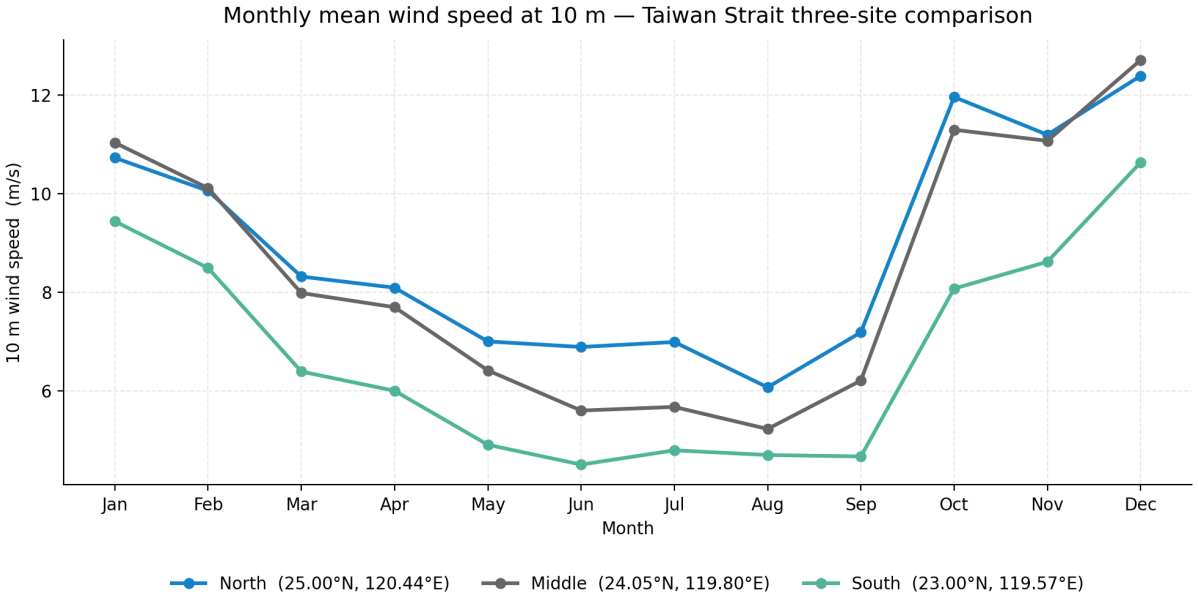

Figure 2: Monthly mean 10 m wind speed at three Taiwan Strait sites — North (25.00°N, 120.44°E, blue), Middle (24.05°N, 119.80°E, grey), South (23.00°N, 119.57°E, green). ERA5 hourly 2019–2023, scalar |U| computed at hourly resolution then aggregated to monthly means, bilinear interpolation at each site. The clean N→S annual gradient and the similar winter / summer N–S spread are consistent with northeast-monsoon dynamics strengthening northward along the Strait.

3.3 Wind direction — three-site comparison

All three sites are dominated by the northeast quadrant (N–NE sector, ~10°–60° FROM-direction), consistent with the East-Asian winter NE monsoon. The circular-mean FROM-direction is ~35° at North, ~22° at Middle, and ~19° at South — Middle and South align along the NNE channel axis (~19–22°), while North sits ~13° further N (more N–NNE) at the open northeastern exit of the Strait.

- **North** shows the widest spread of the three, including a noticeable southwesterly contribution (consistent with summer SW-monsoon exposure at the Strait's northeast exit) and a more N-tilted dominant direction (~35° FROM) than the other two sites.
- **Middle** is the most tightly concentrated in the NNE sector — the largest single sector accounts for roughly 40%+ of all hours — with a circular-mean direction of ~22° FROM aligned along the channel axis.
- **South** has a similar circular-mean direction to Middle (~19° FROM) but lower magnitudes overall, consistent with the southern Strait being further from the NE-monsoon source and partially in the lee of the Penghu Islands for NNE-incident wind.

This directional structure is consistent with the channel-funnelling hypothesis introduced in §3.1 (the middle site's lower mean but higher p95 reflects a directionally-concentrated, episodically-intense regime). The wind-direction–wave-direction offset table is in §4.3 ($\Delta\theta$ table); a more quantitative directional-stability metric (e.g., variance fraction in the dominant sector) is appropriate follow-up work and is out of scope here.

→ See **Figure 3**.

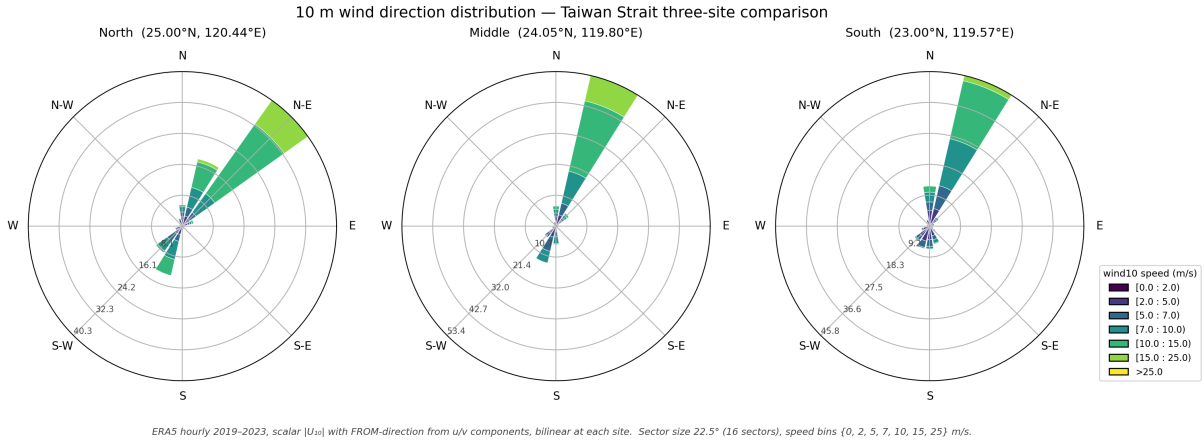

Figure 3: Three-site 10 m wind direction roses — North (left, 25.00°N/120.44°E), Middle (centre, 24.05°N/119.80°E), South (right, 23.00°N/119.57°E). ERA5 hourly 2019–2023, scalar $|U_{10}|$ with FROM-direction derived from u/v components, bilinear interpolation at each site. Sector size 22.5° (16 sectors); speed bins {0, 2, 5, 7, 10, 15, 25} m/s.

---

4. Climatology — wave

4.1 Annual statistics — three-site comparison

Table 6: Three-site annual wave statistics — total significant wave height (Hs, WAVERYS VHM0) and peak wave period (Tp, WAVERYS VTPK), 3-hourly bilinear-interpolated to each site coordinate. n = 14,608 3-hourly samples per site over 2019–2023.

Site	n	Hs mean (m)	Hs p95 (m)	Hs p99 (m)	Hs max (m)	Tp mean (s)	Tp p95 (s)
North (25.00°N, 120.44°E)	14,608	1.60	3.51	4.33	6.13	6.73	9.59
Middle (24.05°N, 119.80°E)	14,608	1.59	3.78	4.66	6.25	6.56	9.18
South (23.00°N, 119.57°E)	14,608	1.35	2.87	3.68	7.65	6.84	9.33

The Hs annual mean is essentially tied at the two northern sites — **N (1.60) ≈ M (1.59) m** — with **South at 1.35 m (~16% below)**. At the tail, the N–M ordering inverts: **M (p99 4.66 m) > N (p99 4.33 m)**, with Middle leading by ~8%. This tail-ordering inversion is the channel-funnelling signature also seen in the wind p95 (§3.1): the central Strait's directionally-concentrated wind regime produces larger waves at the tail despite a marginally lower mean wind. The gap to South is ~15% below N at p99 and ~18% below N at p95. The absolute 5-year max Hs at South (7.65 m) is markedly higher than at N (6.13) or M (6.25) — attributed by timestamp coincidence to **DOKSURI 2023** at 62 km closest pass on 2023-07-27 18:00 UTC (see §6.1 for the per-site catalogue). The simultaneous WAVERYS state at South at that timestamp records

Tp = 11.8 s and wave FROM-direction 159° (SSE); the 159° bearing is consistent with long-fetch swell propagating from the South China Sea / Luzon Strait ahead of and during DOKSURI's transit, rather than with the storm's instantaneous position relative to the site. A method-level caveat: the WAVERYS 0.2° bilinear stencil at 23.00°N / 119.57°E includes grid cells that may partially overlap the Penghu Bank bathymetry (depths ~20–40 m), so the 7.65 m extreme could be partly shaped by shallow-water enhancement that the 0.2° resolution does not fully resolve.

Tp differs from Hs in its site ordering. At the mean, **S (6.84 s) > N (6.73 s) > M (6.56 s)**; at the p95, **N (9.59 s) > S (9.33 s) > M (9.18 s)**. Both the North and South sites have elevated Tp relative to the Middle, consistent with long-period swell exposure at the two end sites: N is at the northeast exit of the Strait, open to East-China-Sea swell propagation; S is south of Penghu, open to swell from the southern Strait / South-China-Sea boundary. The Middle site, in the central Strait within the channel-funnelling region, is dominated by short-fetch wind-sea (locally generated) with a tighter Tp distribution. A partition-Tp diagnostic (separating wind-sea VTM01_WW from swell VTM01_SW1) resolves this directly; see §4.5 for the per-site partition decomposition that delivers the wind-sea vs swell energy split and the SW1 direction roses.

4.2 Seasonal cycle — three-site Hs overlay

The Hs seasonal cycle (Figure 4) shows all three sites peaking in December (M 2.72 m, N 2.51 m, S 2.11 m monthly mean) with summer minima in June (M 0.74 m, S 0.85 m, N 0.95 m). The Middle and North sites track each other closely from October through March, with Middle ~0.2 m above North in the deepest winter months — consistent with the channel-funnelling tail signature that drives the §4.1 p99 ranking. The South site is consistently below both in winter (~0.4 m lower), but notably surpasses Middle in midsummer — South 1.02–1.18 m vs Middle 0.79–0.90 m in July–August — suggesting non-trivial summer Hs at South from southwesterly swell exposure that the more sheltered Middle site does not see. Project work seasons matter: a summer-weighted programme finds the three sites much closer to comparable than the annual mean suggests, with South having the highest summer Hs.

→ See **Figure 4**.

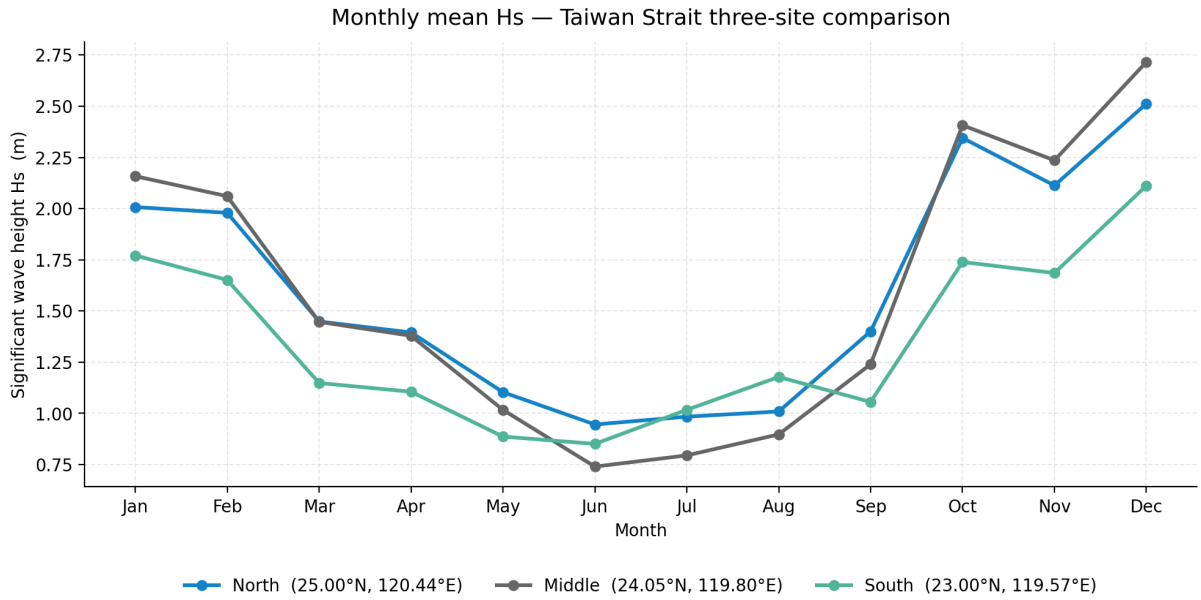

Figure 4: Monthly mean Hs at three Taiwan Strait sites — North (25.00°N, 120.44°E, blue), Middle (24.05°N, 119.80°E, grey), South (23.00°N, 119.57°E, green). WAVERYS multiyear reanalysis 3-hourly 2019–2023, total Hs (VHM0) bilinear-interpolated to each site. Winter peak monthly mean ~2.7 m at Middle, ~2.5 m at North, ~2.1 m at South; summer minima ~0.7–1.0 m, with South above Middle in midsummer (SW-monsoon swell exposure).

4.3 Wind–wave directional relationship

The R3 joint wind-wave alignment (§2.3) now lets us compute, per site, the directional offset $\Delta\theta$ = wave_FROM − wind_FROM (wrapped to (−180°, 180°]) instant-by-instant on the 3-hourly grid and then circularly average. Both quantities use the meteorological FROM convention (§2.4) so $\Delta\theta$ is a direct measurement of the wave field's directional alignment with the forcing wind.

Table 7: Per-site circular mean of $\Delta\theta$ over the joint 3-hourly samples 2019–2023. Sign convention: positive $\Delta\theta$ means the wave FROM direction is rotated clockwise from the wind FROM direction. Hs-weighted mean down-weights low-Hs swell episodes and emphasises the energetic part of the record.

Site	$\Delta\theta$ circular mean	$\Delta\theta$ Hs-weighted mean
North (25.00°N, 120.44°E)	**+2.4°**	**+1.1°**
Middle (24.05°N, 119.80°E)	**+3.4°**	**+2.9°**
South (23.00°N, 119.57°E)	**+4.9°**	**+2.9°**

All three sites show **tight directional alignment** between the total wave field and the forcing wind: the unweighted circular mean of $\Delta\theta$ is between +2.4° and +4.9°, with the Hs-weighted mean tighter at +1.1° to +2.9°. The small southward-increasing $\Delta\theta$ gradient is at the boundary of this metric's resolution and is most parsimoniously read as a combination of site geometry, seasonal swell-source direction, and sample composition rather than as a single physical mechanism.

A small total-wave $\Delta\theta$ does not establish absence of swell. It only establishes that the time-mean wave-energy direction is close to the wind direction. The $\Delta\theta$ *distribution* in fact has a long tail at every site — 9.2% (North), 9.4% (Middle) and 11.2% (South) of 3-hourly samples have $|\Delta\theta| > 90°$ (essentially perpendicular or reversed); but these samples are dominated by **calm episodes** (mean Hs 0.56–0.75 m, mean wind 2.8–3.4 m/s) where the local wind is too weak to align the wave field and any residual swell holds whatever direction it happens to have. Hs-weighting de-emphasises these episodes precisely because their Hs contribution is small, which is why the unweighted circular mean (+2.4° to +4.9°) collapses to a much smaller Hs-weighted value (+1.1° to +2.9°). For the operationally energetic part of the record, the alignment is therefore tight. At the North site, East-China-Sea swell entering the Strait's northeast exit arrives from a similar NNE bearing to the prevailing NE-monsoon wind, so co-directional swell would not produce a large $\Delta\theta$ even when energetic. At the South site, summer SW-monsoon swell episodes (low-Hs months June–August) sit in the same low-Hs-weighting régime described above and therefore contribute little to the Hs-weighted circular mean even when individual events have larger $\Delta\theta$. The total-direction metric is informative about *off-axis* swell but does not measure swell *energy*; the long-period sample fraction in §4.4 and the partition-Tp diagnostic in §4.5 (separating mean periods of the wind-sea VTM01_WW from the swell VTM01_SW1) carry the energy information directionally — see **§4.5** for the per-site partition decomposition. A fuller customer-specific partition-based operability framework (using partition mean periods VTM01_SW1 in the operability tier definitions instead of total Hs alone) remains appropriate follow-up work in a subsequent engagement.

→ See **Figure 5** for the paired-rose visualisation.

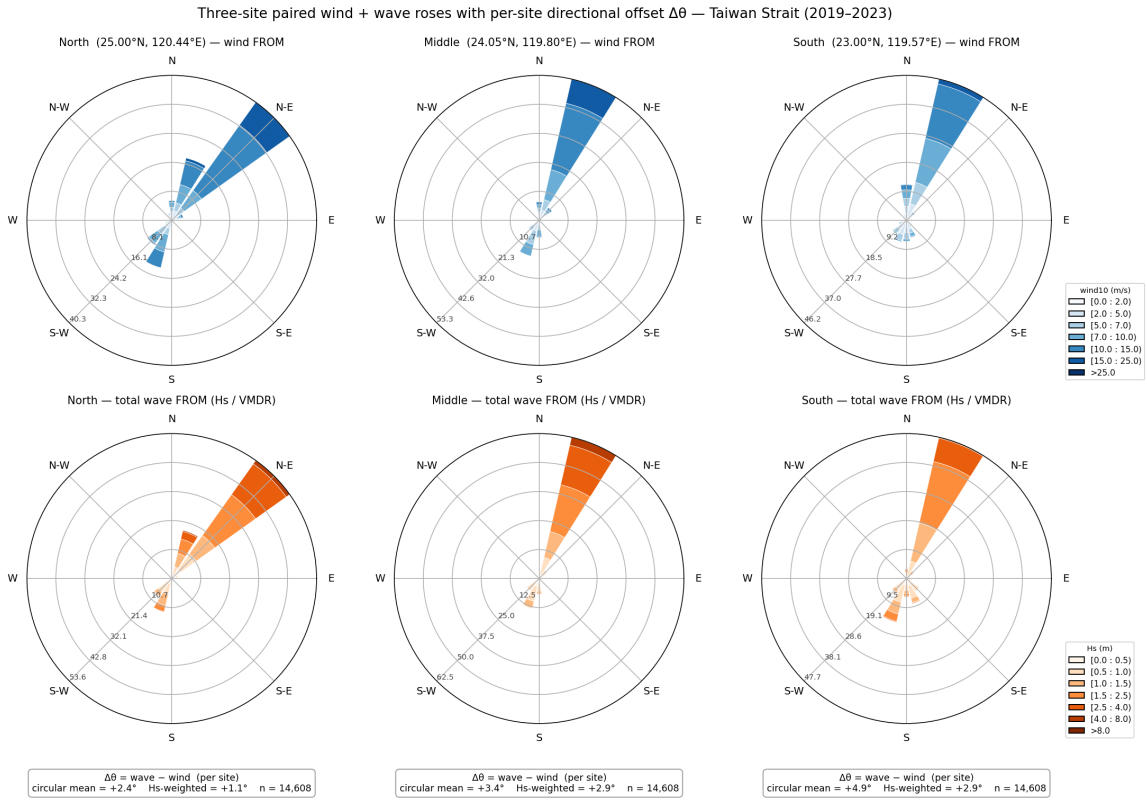

Figure 5: Three-site paired wind + wave roses, Taiwan Strait (2019–2023). Top row: ERA5 10 m wind FROM, per site. Bottom row: WAVERYS total-wave FROM (VMDR weighted by VHM0), per site. Speed bins {0, 2, 5, 7, 10, 15, 25} m/s; Hs bins {0, 0.5, 1.0, 1.5, 2.5, 4.0, 8.0} m; 16 directional sectors (22.5° each). Per-site $\Delta\theta$ statistics (plain + Hs-weighted circular mean, n) are reported in the box below each column. All three sites show NNE-dominated wind and NNE-dominated total wave; the directional alignment is tight (small $\Delta\theta$ at every site).

4.4 Joint Hs–Tp distribution

Per-site hexbin density of significant wave height (Hs, VHM0) versus peak wave period (Tp, VTPK), evaluated on the 14,608 3-hourly samples per site over 2019–2023. The three panels share a single density colour scale and a median-Tp-per-0.25 m-Hs-band overlay; long-period swell band (Tp $\geq$ 10 s) is shaded.

Table 8: Per-site fraction of 3-hourly samples falling in the long-period swell band (Tp $\geq$ 10 s). North leads; Middle is the lowest of the three; South sits in between.

Site	Long-period sample fraction (Tp $\geq$ 10 s)
North (25.00°N, 120.44°E)	**3.5%**
Middle (24.05°N, 119.80°E)	2.1%
South (23.00°N, 119.57°E)	2.9%

The long-period fraction ranks **N > S > M** — consistent with the §4.1 Tp p95 ranking (N 9.59 s > S 9.33 s > M 9.18 s) and with the physical setting: - North sits at the northeast exit of the Strait, open to East-China-

Sea swell propagation; - South sits south of Penghu, open to swell from the open southern Strait / South-China-Sea boundary; - Middle, in the central Strait within the channel-funnelling region, is dominated by short-fetch wind-sea (locally generated) and sees the smallest long-period contribution.

The median-Tp-per-Hs-band overlay shows that across all three sites the per-band median Tp does **not** collapse to the short-fetch wind-sea period limit at low Hs — it sits in the 5–7 s range across the operability-relevant Hs band ($\leq$ 2.5 m). This is consistent with a persistent swell background that holds the spectral peak even when the wind-sea is small, *and* with the §4.6 VTPK switching behaviour in mixed-sea conditions (VTPK is the dominant-peak period, so it picks the swell peak when the swell holds more spectral energy than the wind-sea, regardless of Hs). Threshold note: the "Tp $\geq$ 10 s" cut is a screening shorthand, not a spectral partition — at this latitude and fetch, fully-developed wind-sea Tp during strong NE-monsoon events can reach 9–11 s, so the Tp $\geq$ 10 s sample fraction is an upper bound on the swell-dominated fraction, not a clean swell vs wind-sea decomposition. The §4.3 directional analysis found $\Delta\theta$ small at every site; combined with this §4.4 finding it follows that the long-period swell, where present and energetic, arrives from a similar bearing to the NNE wind-sea — a NNE total-wave field with embedded long-period structure rather than an off-axis swell train — but small $\Delta\theta$ does *not* by itself rule out other swell-source directions when their Hs contribution is low (see §4.3).

→ See **Figure 6** for the per-site joint distribution.

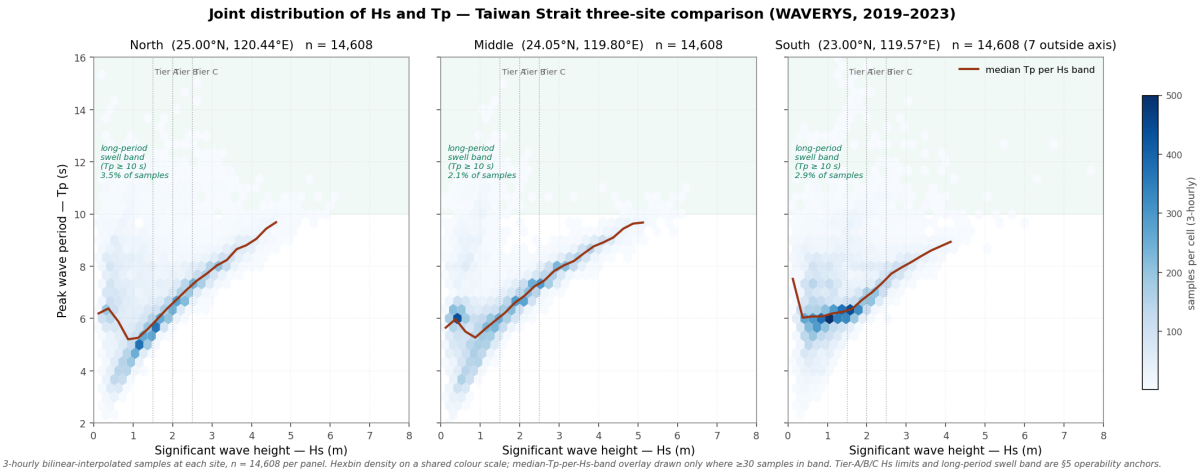

Figure 6: Joint distribution of Hs (VHM0) and Tp (VTPK) at the three Taiwan Strait sites, WAVERYS 2019–2023 (n = 14,608 per panel). Hexbin density on a shared colour scale; orange line = median Tp per 0.25 m Hs band (drawn only where $\geq$30 samples in the band). Vertical dotted lines: Tier A/B/C Hs operability limits (1.5 / 2.0 / 2.5 m). Green band at the top of each panel: long-period swell region (Tp $\geq$ 10 s); the per-site sample fraction in that band is annotated within the band. North shows the highest long-period swell fraction (3.5%); Middle the lowest (2.1%); South in between (2.9%) — consistent with the geographic exposure pattern at the Strait's NE exit (North), central wind-sea regime (Middle), and Penghu-south swell exposure (South).

4.5 Spectral partition — wind-sea vs swell decomposition

South is *not* a "swell-dominated" site in the design-load sense — at extreme events the load is still expected to be wind-sea driven. What this section's partition analysis shows is that on a time-mean basis, almost

half of South's energy comes from southern swell, which makes period-sensitive operations (e.g., crane lifts, motion-sensitive vessels) more sensitive at South than the headline Hs alone suggests.

WAVERYS provides per-component partition variables: wind-sea (`WW`) and two swell trains (`SW1` primary, `SW2` secondary). Decomposing the total wave field into these components, per site, gives a much sharper view of where the swell sits in the cross-segment picture than the §4.3 total-direction analysis or the §4.4 long-period (Tp $\geq$ 10 s) fraction can on their own.

Per-site **wave-energy partition** (per-sample mean fraction of Hs² in each component, 2019–2023):

Table 9: Per-site annual partition statistics from WAVERYS partition variables (VHM0_WW / VHM0_SW1 / VHM0_SW2 + VMDR_SW1 + VTM01_SW1). Energy fractions are computed as mean per-sample component Hs² ÷ total Hs². The 3 fractions sum to ~93% at each site — the residual ~7% is the WAM/WW3 partition-bin-assignment behaviour disclosed in §8.1 item 4 (this is not a data error, just the spectral-partition arithmetic). SW1 mean Hs and Tm01 are computed over samples with non-zero SW1 only.

Site	Wind-sea (WW)	Primary swell (SW1)	Secondary swell (SW2)	SW1 direction circular mean	SW1 Hs-weighted mean direction	SW1 mean Hs (m)	SW1 mean Tm01 (s)
North	58.3%	29.2%	6.4%	46° (NE)	45° (NE)	0.48	7.22
Middle	54.1%	31.3%	7.8%	59° (NE)	41° (NE)	0.46	6.86
South	**35.0%**	**47.9%**	10.3%	99° (E)	**138° (SE)**	0.67	6.60

The headline differential is **at the South site**: the primary-swell partition (SW1) carries **47.9%** of the time-mean wave energy, **exceeding the wind-sea contribution (35.0%)**, so SW1 is the largest single energy component at South over the 2019–2023 record. North and Middle, by contrast, are both wind-sea-leading (WW ~55%) with SW1 around 30%. The "swell-leading" partition signal at South describes the 5-year time-mean energy budget; during the operationally-critical winter-monsoon and typhoon events the wind-sea component is expected to dominate instantaneous Hs (see the Reconciling paragraph below), so this is a swell-character signal, not a statement that swell drives the design-load envelope at South.

SW1 direction reinforces the same finding. At North and Middle, SW1 arrives from a near-NE bearing (circular mean 46° and 59°; Hs-weighted 45° and 41°) — close to the prevailing NNE wind direction (§3.3) and therefore not separable from it by a total-wave-direction metric like §4.3's $\Delta\theta$. At South, SW1 has a circular mean direction of 99° (E) and an Hs-weighted mean of **138° (SE)** — materially off-axis from the local NNE wind (~19°). This Hs-weighted SE bearing is consistent with swell propagation from the southern Strait / South-China-Sea boundary into the southern Strait, and is exactly the swell exposure suggested by South's geographic position south of Penghu Islands.

→ See **Figure 7** for the per-site SW1 direction roses.

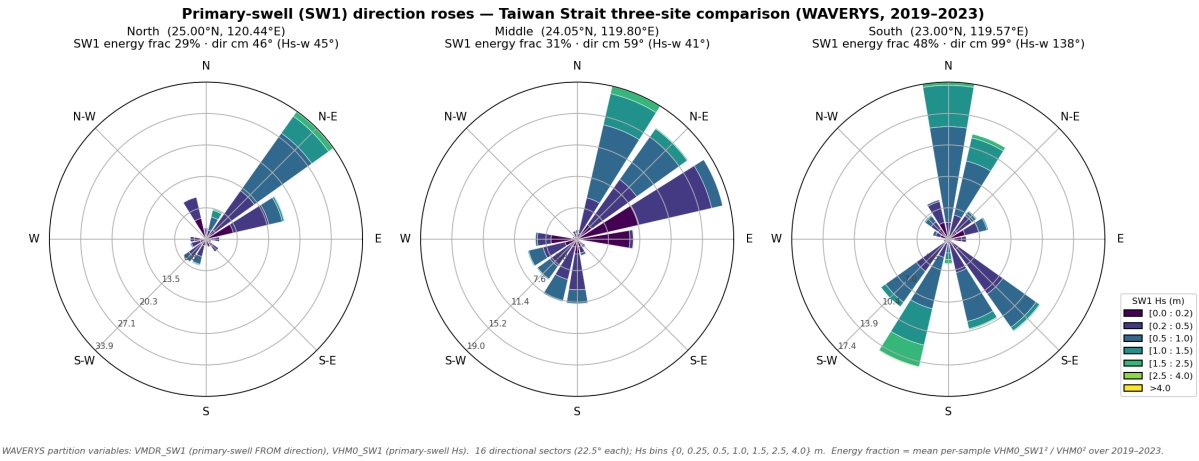

Figure 7: Primary-swell (SW1) direction roses at the three Taiwan Strait sites, WAVERYS 2019–2023. Each panel shows the partition VHM0_SW1 / VMDR_SW1 distribution on 16 directional sectors (22.5° each) and Hs bins {0, 0.25, 0.5, 1.0, 1.5, 2.5, 4.0} m. Panel titles report the SW1 energy fraction (per-sample mean of VHM0_SW1² / VHM0²) and the SW1 direction circular mean (plain and Hs-weighted). North and Middle both show NE-concentrated SW1 (largely co-directional with the local NNE wind, §3.3); South shows a much broader spread with substantial S, SSE, SE and E contributions — physically consistent with swell exposure from the open south through the Strait's southern boundary.

Reconciling §4.3, §4.4 and §4.5. A reader may notice an apparent tension between (a) §4.3's finding that the Hs-weighted total-wave $\Delta\theta$ is small at every site ($\leq$ +2.9°), (b) §4.4's modest long-period Tp $\geq$ 10 s sample fractions (2.1–3.5%), and (c) §4.5's finding that SW1 is the largest single energy component at South (47.9%, exceeding WW at 35.0%). These are all consistent. The total-wave direction is the energy-weighted average of *all* wave components, so when wind-sea and SW1 share similar bearings (as at North and Middle), the total direction stays near the wind direction even if SW1 carries 30% of the energy. At South, SW1 carries 48% of energy but its Hs-weighted mean direction is SE (~138°), almost perpendicular to the NNE wind-sea bearing — yet the energetically-largest samples are still typhoon and winter-monsoon events where wind-sea and wind-driven swell jointly produce NNE-aligned waves; those events dominate the Hs-weighted $\Delta\theta$ even though SW1 swell is the dominant energy fraction over the full record. The §4.4 long-period (Tp $\geq$ 10 s) threshold, meanwhile, is a *peak-period* criterion (VTPK); South's SW1 has mean Tm01 = 6.60 s and is mostly below the 10 s peak threshold. A swell-aware operability framework (out of scope for Level 1; see §8.4 item 15) would use partition-energy and partition-period fields directly rather than VTPK alone.

4.6 Wave climatology caveat

The Hs values in §4.1 and §4.2 are total significant wave height (WAVERYS VHM0). The peak period Tp shown in §4.1 is WAVERYS VTPK, the spectral *peak* period. **Tp-metric caveat for motion-sensitive work**: in mixed-sea conditions (wind-sea and swell coexisting with comparable energy — exactly the regime documented in §4.5 across all three sites and particularly at South), VTPK can switch between the wind-sea peak and the swell peak even when total Hs barely changes — so VTPK alone can mis-state the period a vessel actually responds to. For motion-sensitive operations (crane envelope, CTV transfers, floating-asset

response) the cleaner descriptor is a partition mean period (e.g. VTM01_SW1 as in §4.5) or the motion-relevant Te / Tm-1,0. VTPK is used here as the standard quick-look descriptor; the partition variables are present in the per-site Parquets and were used in §4.5.

Reminder of the typhoon-period caveat from §2.5: peak Hs values at any of the three sites during typhoon passages should be treated as **indicative, not design-level**, due to known low ERA5 wind bias for compact intense TCs.

---

5. Operability

5.1 Joint-frame operability — three-site comparison

Per-site annual fraction of 3-hourly samples meeting **both** Hs and wind10 thresholds simultaneously at three illustrative offshore-wind tiers (n = 14,608 per site over 2019–2023).

Table 10: Annual joint-frame operability fractions and equivalent operable days per year (≈365 d/yr × pct). The South site leads all three tiers. The N–M ranking inverts at the robust tier: at A and B, Middle slightly exceeds North; at C the North site overtakes Middle, reflecting that the channel-funnelling regime at the central Strait pushes the wave-tail above the 2.5 m threshold more frequently than at North. Tier-B (Hs $\leq$ 2 m, wind $\leq$ 12 m/s) is the canonical offshore-wind operability threshold; the South site's ~12-percentage-point lead (~48 d/yr more standard-ops time) is the headline operability finding.

Tier	Hs limit	wind10 limit	North % (days/yr)	Middle % (days/yr)	South % (days/yr)
A — sensitive ops	$\leq$ 1.5 m	$\leq$ 10 m/s	50.1% (183)	55.8% (204)	**63.9% (233)**
B — standard ops	$\leq$ 2.0 m	$\leq$ 12 m/s	67.2% (245)	67.9% (248)	**80.3% (293)**
C — robust ops	$\leq$ 2.5 m	$\leq$ 15 m/s	81.0% (296)	78.7% (287)	**90.5% (331)**

5.2 Persistence run-length distribution

The percentiles below describe **individual continuous-run durations**: for each contiguous block of 3-hourly samples staying operable (or staying non-operable) the block's duration enters the corresponding distribution; *p90 is the 90th percentile of those episode durations.* The operability percentages above hide this temporal structure — 56% operability split into many short windows is operationally worse than the same fraction delivered as long stretches. At Tier B (standard ops, Hs $\leq$ 2 m AND wind10 $\leq$ 12 m/s):

Table 11: Tier-B per-site operable and downtime run-length statistics over 2019–2023 (Hs $\leq$ 2 m AND wind10 $\leq$ 12 m/s, 3-hourly samples). All quantities in hours; n is the count of distinct continuous runs.

Site	Operable runs (n, median h, p90 h, max h)	Downtime runs (n, median h, p90 h, max h)
North	349, 36, 197, 1,119	350, 21, 90, 558
Middle	287, 36, 204, **2,535**	288, 27, 106, 531
South	310, **39**, **298**, 1,206	311, **15**, **63**, 291

The South site is best on every persistence statistic except the single longest operable run. South's median non-operable episode is **~15 hours** (about 5 consecutive 3-hourly samples) versus 21 h at North and 27 h at Middle — meaning a typical bad-weather episode at South returns to operable within a working day. South's p90 non-operable episode duration is **63 hours** versus 90 h (North) and 106 h (Middle) — at South, 90% of bad-weather episodes resolve within 63 h, ~30% shorter than at North and ~40% shorter than at Middle. The Middle site has the longest single uninterrupted operable run on record at 2,535 hours (~106 days, mid-2022 calm), but this is an outlier; the median and p90 favour South.

→ See **Figure 8** for the per-tier survival curves.

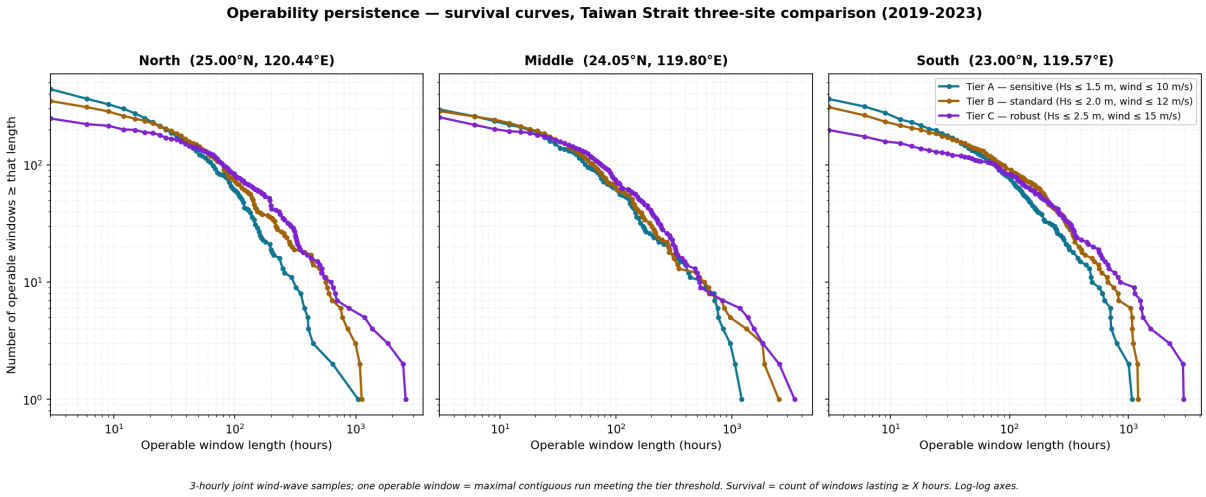

Figure 8: Operability persistence — survival curves for the three Taiwan Strait sites (2019–2023). One panel per site, each showing three tier curves: Tier A (sensitive, teal), Tier B (standard, ochre), Tier C (robust, purple). Log-log axes; one operable window = maximal contiguous run of 3-hourly samples meeting the tier threshold. South's curves sit consistently to the right of the North and Middle equivalents at the upper end (more long-duration operable windows); Middle shows the longest single-event tail at all three tiers (visible as the far-right plateau).

6. Cross-segment differential analysis

6.1 Typhoon exposure — three-site catalogue

IBTrACS v4r01 storm tracks were filtered to systems whose tracks passed within **200 km of any site** during 2019–2023 with **peak lifetime intensity ≥ Tropical Storm (34 kt)**. Distance metric: haversine great-circle. The extraction reads the full IBTrACS archive directly (no spatial pre-filter) and applies the basin (Western Pacific, evaluated at first track point) + season + lifetime-peak + 200 km filters at storm level; this avoids any extent-driven completeness gap at the North / South 200 km filter circles. Saffir-Simpson categories are based on the JTWC 1-minute sustained wind field (`usa_wind` in IBTrACS) — the standard 1-min basis for the SS scale — rather than the WMO 10-minute basis. See §8.2 item 8 for the catalogue-completeness boundary documentation.

Table 12: Three-site typhoon exposure catalogue. Unique-storm union across all three sites is nine: LUPIT 2021 and DOKSURI 2023 touch all three; HAIKUI 2023, ATSANI 2020, BAILU 2019, MEKKHALA 2020 touch Middle and South; CHANTHU 2021 (Cat 5 at lifetime peak) touches only North; CHOI-WAN 2021 and KOINU 2023 (Cat 4 at peak, 100 km closest pass) touch only South.

Site	Storms (2019–2023)	Rate (per yr)	Closest pass median (km)	Closest pass min (km)	Peak wind median (kt)	Peak wind max (kt)
North	**3**	**0.6**	186	16	130	**155**
Middle	6	1.2	131	**95**	65	130
South	8	1.6	**81**	23	65	130

The North site has the **lowest typhoon exposure frequency** of the three sites (0.6 storms/yr versus Middle's 1.2 and South's 1.6 — about half the central-and-southern Strait rate); this is physically plausible — Taiwan main-island is a topographic obstacle for westward-tracking systems approaching from the southeast, and storms that recurve over the western Pacific into the East China Sea track east of Taiwan rather than through the northern Strait. When a storm *does* pass close to the North site (LUPIT 2021, 16 km closest pass), the proximity and intensity can be exceptional — North also records the catalogue's only Cat 5 (CHANTHU 2021, 155 kt **lifetime peak**; the storm's intensity at the moment of closest approach to North (189 km) is expected to be below the lifetime peak as the system would have been weakening or far from peak — the SS categories in §6.2 / the Table 11 SS distribution refer to lifetime peak unless otherwise noted). Low exposure frequency does not imply low single-event load. The Middle site has the **largest minimum closest-pass in this 5-yr catalogue (95 km)**: no storm during 2019–2023 passed closer than 95 km to Middle. This minimum-comparison metric is sample-size sensitive — Middle's minimum is drawn from six events versus North's three — and should not be read as a stable geometric "shelter" claim. The South site has the highest exposure rate (1.6 storms/yr), with both the closer median pass (81 km) and the closest-of-record HAIKUI 2023 at 23 km; KOINU 2023 (Cat 4 lifetime peak, 120 kt) passed within 100 km of the South site, reinforcing the southern Strait's stronger typhoon exposure relative to the other two sites.

→ See **Figure 9** for the regional tracks map.

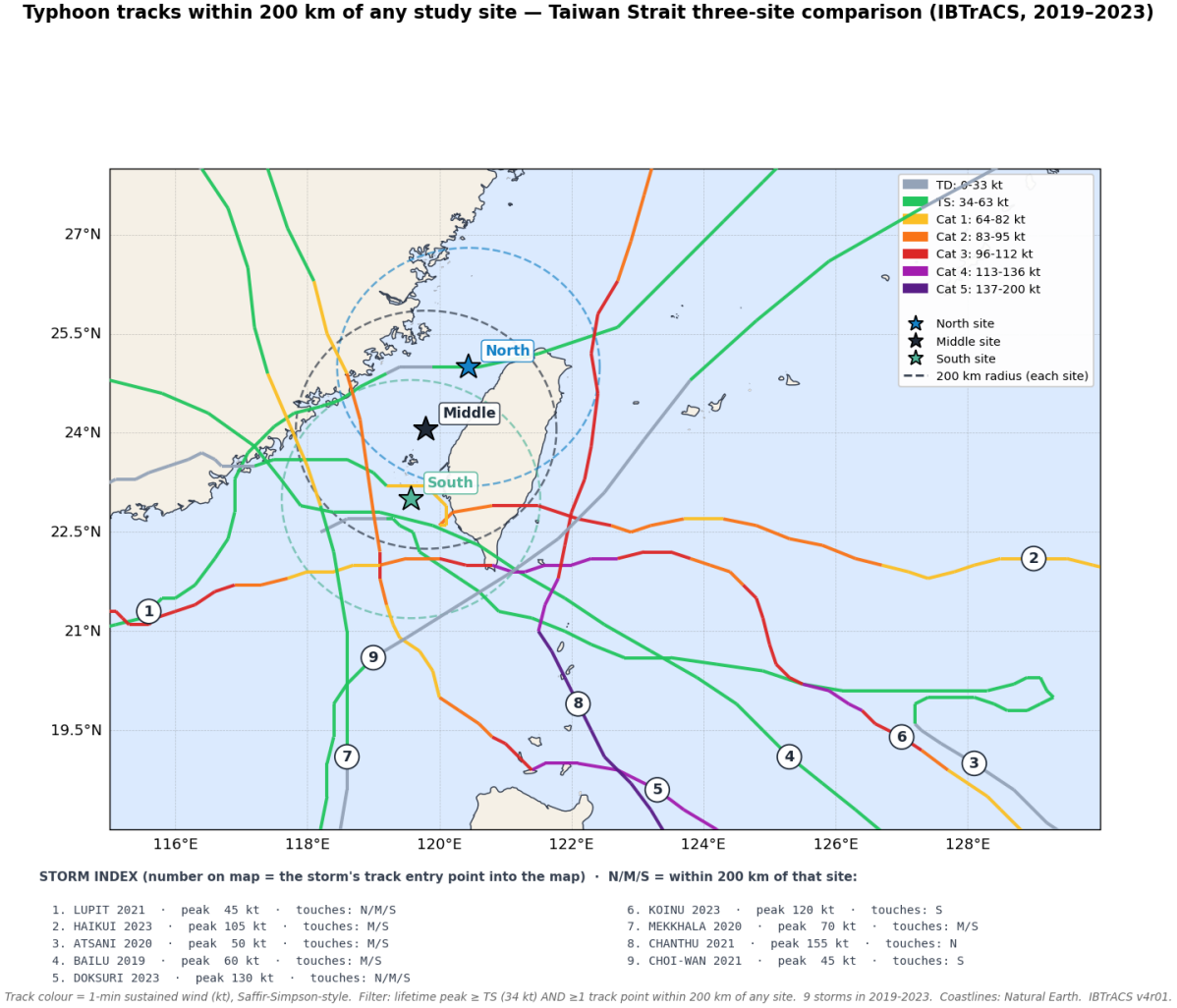

Figure 9: Typhoon tracks within 200 km of any of the three study sites over 2019–2023 (IBTrACS v4r01, filter: storms whose **lifetime peak** intensity reached ≥ TS 34 kt). Nine unique storms shown; track colour = 1-min sustained wind on a Saffir-Simpson-style scale evaluated at each individual track point — pre-intensification segments of qualifying storms therefore appear in the TD colour band (0–33 kt), but every storm displayed satisfies the lifetime-peak filter. Three sites marked (North blue, Middle dark grey, South green) with 200 km dashed filter circles colour-matched to each site. Numbered markers sit directly on each track at the storm's first track point inside the map, identifying which track corresponds to which storm in the index; the storm index at the bottom lists name + year + peak intensity + which sites the storm touched (N / M / S). Coastlines from Natural Earth.

6.2 Critical-parameter differential summary

The §3–§5 results and the §6.1 catalogue are synthesised into a single ranking table below. **Spread %** = (max − min) / median × 100, an order-of-magnitude proxy for how much the three sites differ on each metric. **Intent** indicates the direction in which "best" lies (`max` = higher is better, e.g. wind resource; `min` = lower is better, e.g. extreme load). Rank 1 (bolded value) is best for the metric's intended use.

Table 13: Cross-segment critical-parameter differential summary, ranked by metric. Bold = rank 1 for the metric's intended use. Wind p95 and wind p99 carry opposite Intent because they target different decision frames: p95 represents the upper operating tail (more time near or above rated wind speed; `max` = greater rated-band exposure), while p99 represents high-wind load exposure on structures (`min` = lighter load). Capacity factor itself is governed by the full wind-speed distribution and turbine power curve, not by the upper tail alone. "Tier-B operable run max" (Middle 2,535 h, North 1,119 h, South 1,206 h) is intentionally excluded — its spread % is driven by Middle's single mid-2022 outlier and is not directly comparable to median-based discriminators; that statistic is reported in the §5.2 table instead. **5-year absolute maxima (Hs max, wind10 max) and typhoon "closest-pass min" / "exposure rate" are event-sampled within the 2019–2023 catalogue and are not rank-stable across resampling** — they should be read as catalogue-period statistics rather than climatology. Typhoon "closest-pass min" in particular has very high apparent spread because it compares minimums across unequal samples (N=3 at North vs N=6 at Middle and N=8 at South).

Metric	Units	Intent	North	Middle	South	Spread %	Best
Annual mean wind10	m/s	max	**8.91**	8.42	6.77	25.4	**N**
Wind10 p95	m/s	max	15.82	**16.19**	13.64	16.2	**M**
Wind10 p99	m/s	min	17.52	18.24	**15.74**	14.1	**S**
Wind10 max (5-yr)	m/s	min	**23.79**	24.09	25.56	7.3	**N**
Annual mean Hs	m	min	1.60	1.59	**1.35**	15.9	**S**
Hs p99	m	min	4.33	4.66	**3.68**	22.7	**S**
Hs max (5-yr)	m	min	**6.13**	6.25	7.65	24.3	**N**
Tier-A operability	%	max	50.1	55.8	**63.9**	24.7	**S**
Tier-B operability	%	max	67.2	67.9	**80.3**	19.3	**S**
Tier-C operability	%	max	81.0	78.7	**90.5**	14.6	**S**
Tier-B operable run median	h	max	36	36	**39**	8.3	**S**
Tier-B non-op episode p90	h	min	90	106	**63**	47.7	**S**
Typhoon exposure rate	/yr	min	**0.6**	1.2	1.6	83.3	**N**
Typhoon closest-pass min	km	max	16	**95**	23	335.6	**M**

6.3 Site-screening synthesis

None of the three sites is "best" overall. North is the windiest with the fewest typhoons in this window; South is calmest with the most operable days but the most typhoons; Middle sits between the two on most axes but carries the largest p99 Hs from channel funnelling. Which site is "best" depends entirely on which axis matters most for the project — the right reading is *cross-segment trade-off thinking*, not single-number ranking.

No single site dominates across all axes. Single-parameter ranking is misleading at the screening level: the picture is a structured three-way trade-off.

- **North** is best for *mean wind resource* (8.91 m/s, ~5% above Middle and ~32% above South) and best for *typhoon-exposure frequency* (~0.6 storms/yr, about half of Middle's 1.2 and ~40% of South's 1.6). It is also tied-best on both 5-year absolute maxima: *Hs max* (6.13 m, marginally below Middle's 6.25 m) and *wind10 max* (23.79 m/s, ~0.3 m/s below Middle and ~1.8 m/s below South) — though the absolute-max ranking is sample-event statistics with high uncertainty (§8.2 item 10). Tradeoff: North's operability fraction at the sensitive and standard tiers is the lowest of the three, and two close-to-Cat-4-or-higher typhoons in the 5-yr window (LUPIT 2021 at 16 km, CHANTHU 2021 at 189 km with 155 kt peak — the catalogue's only Cat 5) show that low exposure frequency does not imply low single-event load. North is **the wind-resource site**.
- **Middle** carries the *largest p95 / p99 wind tail* and the *channel-funnelling Hs tail signature* (highest p99 Hs at 4.66 m). It holds the *largest single Tier-B operable run on record* (2,535 hours, mid-2022 outlier) and **the largest minimum typhoon closest-pass in this 5-yr catalogue (95 km)** — no storm during 2019–2023 passed closer than 95 km to Middle (a sample-size-sensitive metric: drawn from six events vs three at North and eight at South). Tradeoff: highest p99 Hs combined with the second-highest typhoon rate is the dominant load signature; the closest-pass minimum is a soft cushion, not a stable geometric shelter.
- **South** leads on the *operability axis*: best on every operability tier, best on the operable-run median, and best on non-operable-episode persistence (median 15 h; p90 episode duration 63 h, ~30% shorter than at North's 90 h and ~40% shorter than at Middle's 106 h). South is also calmest at the *mean Hs* (1.35 m). Tradeoff: South is **swell-leading at the time-mean energy level** (SW1 partition 47.9% versus wind-sea 35.0%; §4.5) with Hs-weighted swell direction at 138° (SE) — materially different from the local NNE wind — which makes motion-sensitive operations more period-sensitive than the headline Hs alone would suggest (the design-load envelope is still expected to be wind-sea-driven at extreme events; see the §4.5 Reconciling paragraph). South also carries the **highest *Hs absolute 5-year maximum*** (7.65 m, attributed to DOKSURI 2023 at 62 km closest pass on 2023-07-27 — see §4.1; the §4.6 caveat about Penghu Bank bathymetry holds at South), and the **highest typhoon exposure rate (1.6 / yr)** of the three sites in this catalogue; when typhoons do reach the southern Strait they tend closer (median 81 km versus Middle's 131 km), with KOINU 2023 (Cat 4, 100 km closest pass) the second-most-recent Cat-4+ event at South.

Screening implication. A development decision keyed on *mean wind energy yield alone* picks North; a decision keyed on *standard-tier operability % alone* picks South; a decision keyed on *typhoon exposure frequency alone* also picks North; a decision keyed on *closest-pass cushion in the 2019–2023 sample alone* picks Middle. The single-parameter rankings disagree, and that is the value of the cross-segment differential view at screening: it makes the trade-off **explicit** rather than embedded in a single number. None of these reduce to a formal design-load envelope — that requires per-event TC attribution and extreme-value analysis, both out of scope here. The next level of refinement (per-event TC attribution; partition-Tp swell vs wind-sea decomposition; per-site bathymetry sensitivity at South; formal extreme-value analysis for design loads) is **out of scope for this desktop-study report** and requires a follow-up engagement with dedicated dataset acquisition.

---

7. Cross-validation against open observational data

This section asks whether the WAVERYS numbers used in §3 – §6 are broadly reasonable, by cross-checking them against an independent 10-year climatology (CWA WW3) and against two CWA buoys over a recent 30-day window. The seasonal pattern checks out; absolute magnitudes and extreme values do not — those require in-situ buoy data at the site and formal extreme-value analysis, which are outside this report's scope.

This section is a **consistency check, not a formal model validation or bias-correction exercise**. It cross-checks the WAVERYS multiyear-reanalysis Hs used in §3 – §6 against two open-licence sources from the Central Weather Administration (CWA) of Taiwan: §7.1 is a model-vs-model seasonal-cycle check against the CWA WW3 10-yr hindcast at all three sites; §7.2 is a model-vs-observation buoy check at the two CWA wave-instrumented buoys nearest the three study sites. Both checks preserve a "**supports / consistent with**" tone discipline (in preference to "validates / correctly represents") because (a) the comparisons are between non-overlapping windows and different model variants, (b) at-site historical buoy data is not part of the free CWA OpenData tier (see §8.3 item 12 for scope), and (c) formal validation requires per-event bias-corrected comparison against in-situ instruments at the three study sites — beyond the scope of this desktop-study report.

7.1 Seasonal-cycle consistency — CWA WW3 10-yr vs WAVERYS 5-yr at three sites

CWA's `C-B0086-001` 台灣海域波候統計 (2008-2017 monthly mean / median / max Hs on a 0.25° grid, modelled with WaveWatch III by CWB) is bilinear-interpolated to each of the three study sites coordinate, then compared against the WAVERYS 2019-2023 site monthly aggregates from §4. Two independent wave hindcasts (different model code WW3 vs MFWAM, different forcing CWB internal vs ERA5, different decadal windows). High Pearson r on the **seasonal cycle** is methodological evidence that the WAVERYS reanalysis reproduces the Taiwan Strait wave climatology pattern at all three sites — it does **not** extend to validating absolute magnitudes (the ~0.25 m bias is not small), and it does **not** constitute extreme-value validation.

Table 14: CWA WW3 10-yr (2008-2017) vs WAVERYS 5-yr (2019-2023) monthly Hs cross-check per site. Bias and RMSE use month-pair (W – C); Pearson r is over the 12-month seasonal cycle. Maximum-Hs comparison is not reported in this table because non-overlapping windows make single-event extremes intrinsically noisy.

Site	Statistic	bias (W – C, m)	RMSE (m)	Pearson r (12-month cycle)
North (25.00°N, 120.44°E)	Mean Hs	+0.24	0.27	**0.981**
North	Median Hs	+0.23	0.26	0.968
Middle (24.05°N, 119.80°E)	Mean Hs	+0.25	0.32	**0.970**
Middle	Median Hs	+0.21	0.27	0.964
South (23.00°N, 119.57°E)	Mean Hs	+0.29	0.40	**0.771**

Site	Statistic	bias (W – C, m)	RMSE (m)	Pearson r (12-month cycle)
South	Median Hs	+0.29	0.40	0.902

Seasonal-cycle agreement is strong at all three sites for the mean and median Hs. Mean-Hs r = 0.98 (N) / 0.97 (M) / 0.77 (S): the two end-of-Strait sites (North NE-exit, South Penghu-south) and the central Strait all reproduce the same NE-monsoon-dominated (Oct – Mar) vs SW-monsoon-minimum (Jun – Aug) seasonal cycle in both hindcasts. The South site's r = 0.77 is lower than N / M's r ≈ 0.97-0.98 but still indicates a strongly correlated seasonal cycle; the gap is consistent with South's larger summer SW-monsoon swell contribution (see §4.5 partition decomposition) being more sensitive to inter-decadal SW-monsoon variability between the 2008-2017 (CWA) and 2019-2023 (WAVERYS) windows.

WAVERYS reads **systematically higher** than the CWA WW3 10-yr climatology at all three sites (bias +0.24 to +0.29 m). Two non-exclusive explanations: (a) 2019-2023 was anomalously strong in the NE-monsoon relative to 2008-2017 (the winter-Hs columns of the per-site table show the largest contributions to the bias come from Oct – Dec); (b) WAVERYS / MFWAM has a documented mild positive bias for moderate-to-strong wind-sea regimes (Stopa 2018, multi-hindcast comparison against satellite altimeter SWH; Copernicus Marine Service WAVERYS QUID for `GLOBAL_MULTIYEAR_WAV_001_032`). The bias magnitude is consistent across the three sites (±0.03 m), supporting the methodology-level interpretation that this is a model-family / window-window difference rather than a site-specific issue.

→ See **Figure 10** for the per-site monthly mean Hs comparison.

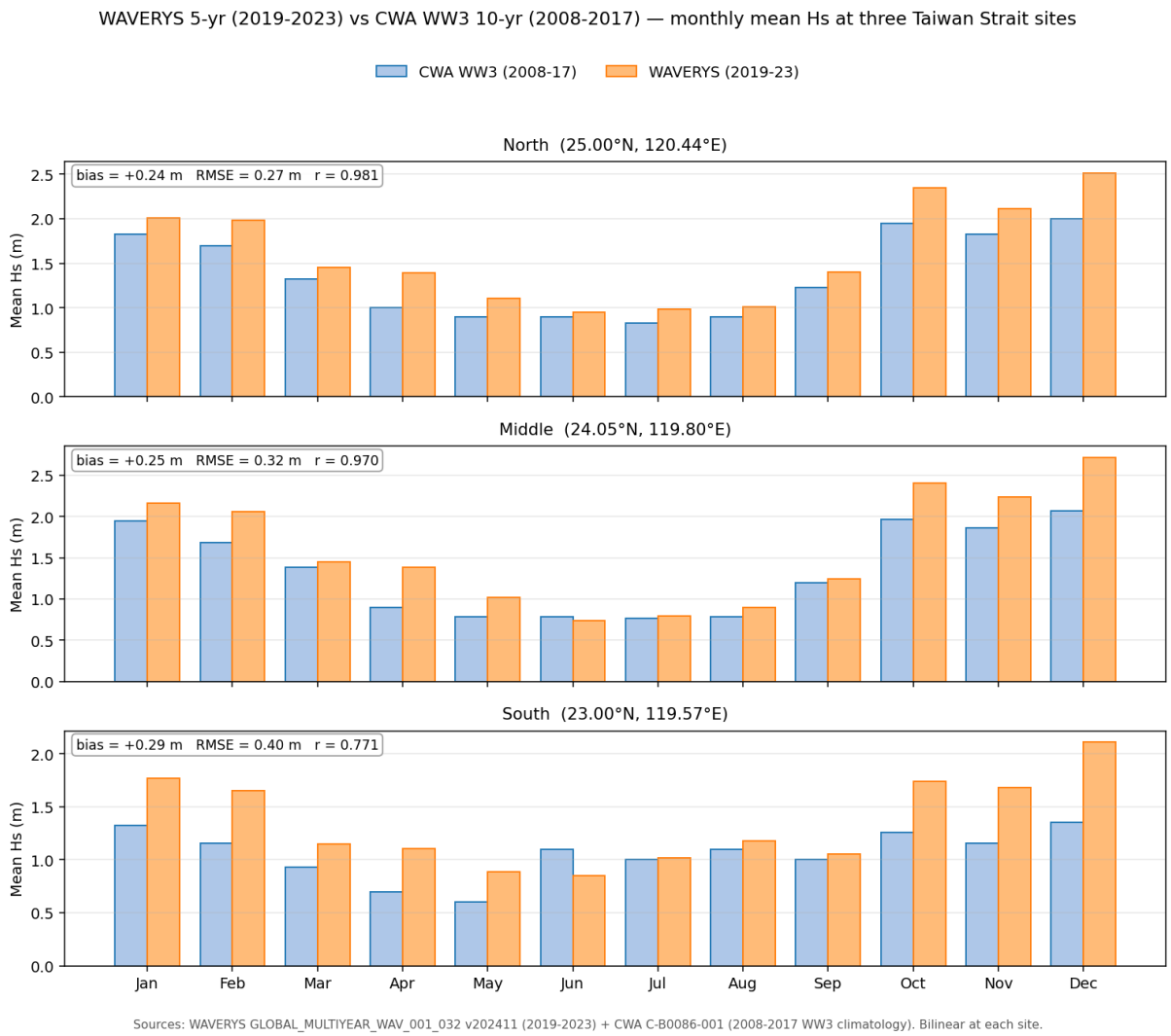

Figure 10: Per-site monthly mean Hs cross-check: WAVERYS multiyear reanalysis (2019-2023, orange) vs CWA WW3 climatology (2008-2017, blue), bilinear-interpolated at each of the three study sites. Top: North (25.00°N, 120.44°E); middle: Middle (24.05°N, 119.80°E); bottom: South (23.00°N, 119.57°E). Per-panel stats box: bias, RMSE, Pearson r over the 12-month seasonal cycle. WAVERYS reads systematically higher than CWA WW3 at all three sites (~0.25 m bias), with seasonal-cycle Pearson r $\geq$ 0.97 at North and Middle and r = 0.77 at South.

7.2 Buoy / WAVERYS-NRT cross-check at the nearest CWA wave buoys

Period note: the §7.2 statistics below were computed over the 30-day rolling window 2026-04-06 → 2026-05-06 from the free `0-B0075-002` tier (the only tier without a 申購 purchase). The window falls in the **spring-transition season** (after the NE-monsoon peak, before SW-monsoon establishment), so the Hs distribution is dominated by low-to-moderate values — the bias / RMSE / r statistics below characterise WAVERYS-family skill in that regime, **not** during the NE-monsoon winter regime that drives the §3–§6 climatology tail. A future rerun on a different 30-day window will produce different per-buoy statistics; this is documented in §8.3 item 12d.

The two CWA wave-instrumented buoys with ≥ 80% wave coverage in this 30-day window are:

Table 15: CWA buoy vs WAVERYS analysis-forecast (`cmems_mod_glo_wav_anfc_0.083deg_PT3H-i`, 3-hourly, 0.083°) cross-check at the two CWA wave buoys with sufficient 30-day coverage. Hsinchu's WAVERYS extraction falls on the coastal land / shallow mask; values are taken from the nearest valid sea cell at (24.75, 120.75) — offset 9.7 km from the buoy. Qimei is bilinear-interpolated directly at the buoy coordinate.

Buoy	Station ID	Coordinate	n (3-hourly aligned)	bias (W – C, m)	RMSE (m)	Pearson r
Hsinchu 新竹	46757B	24.76°N, 120.84°E	229	**-0.01**	0.25	0.847
Qimei 七美	C6W10	23.19°N, 119.65°E	226	**+0.05**	0.23	0.883

For each of the three sites, the nearest CWA wave buoy is:

Table 16: Per-site straight-line distance to the two CWA wave-instrumented buoys used. **South** sits ~22 km from Qimei — the cleanest in-situ check this report carries. **North** sits ~36 km from Hsinchu — also a usable in-situ check. **Middle** has no CWA wave buoy closer than ~96 km — the §7.2 result at the nearest buoy is treated as a supporting check for WAVERYS reliability in the central Strait, not a site-direct measurement, and its strength is reduced by Qimei's 96 km distance and the Penghu Islands sitting between Qimei and Middle (§8.3 item 12).

Site	Nearest CWA wave buoy	Distance	Second-nearest	Distance
North	Hsinchu 46757B	**~36 km**	Qimei	~221 km
Middle	Qimei C6W10	~96 km	Hsinchu	~132 km
South	Qimei C6W10	**~22 km**	Hsinchu	~219 km

Both buoys agree well with WAVERYS-NRT Hs over the 30-day window: Hsinchu RMSE 0.25 m at bias essentially zero (read against the WAVERYS offshore-extraction point at (24.75°N, 120.75°E), 9.7 km west of the buoy — see Table caption above), Qimei RMSE 0.23 m at +0.05 m bias (read at the buoy coordinate directly). Pearson r is 0.85-0.88 at hourly aligned 3-hourly grid — **good tracking of synoptic Hs variability at both buoys within this calm-regime window**; this supports model-family reasonableness for the temporal pattern, not absolute-magnitude or extreme-value validation. Caveat: the WAVERYS analysis-forecast variant used at §7.2 differs from the multiyear reanalysis used in §3 – §6 in its assimilation stream and forcing window, so the §7.2 buoy / model agreement reflects the overall reasonableness of the WAVERYS / MFWAM model series, not the specific bias of the reanalysis variant at the buoys. The §7.1 climatology check, which uses the §3 – §6 reanalysis directly, is the more reanalysis-direct line of evidence.

→ See **Figure 11** for the 30-day Hs tracking time series at both buoys.

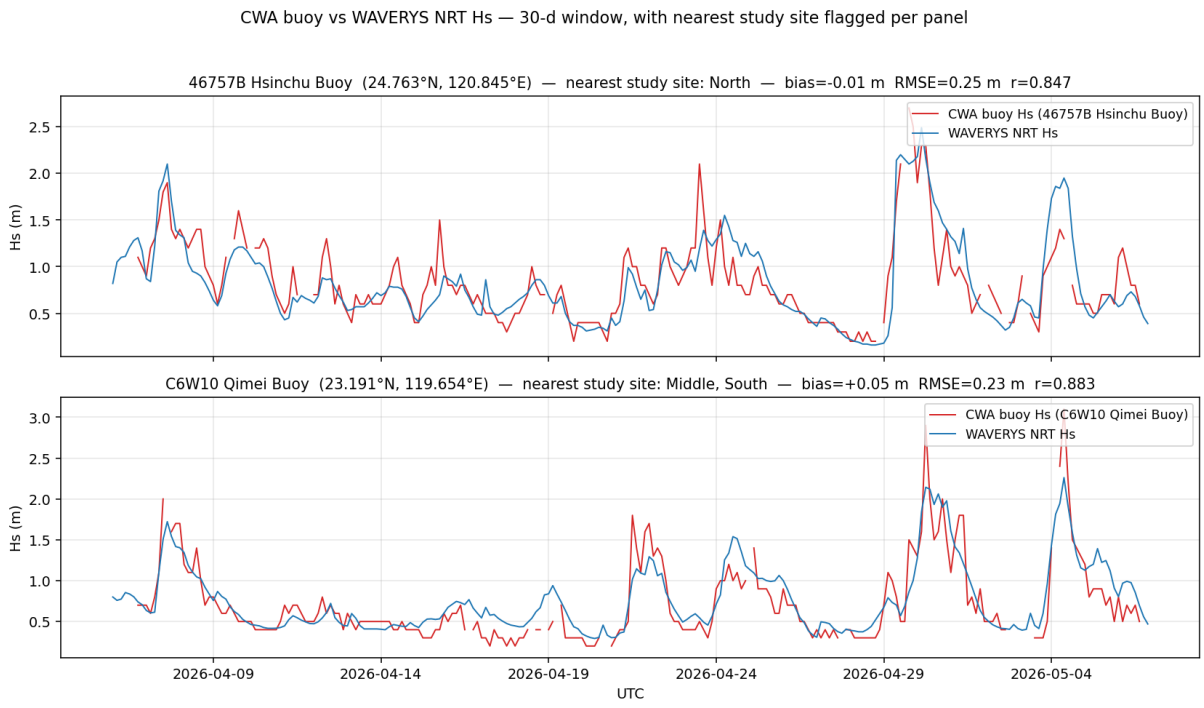

Source: CWA O-B0075-002 (free, rolling 30 d) + CMEMS WAVERYS analysis-forecast (`cmems_mod_glo_wav_anfc_0.083deg_PT3H-i`, 0.083° 3-hourly). Period 2026-04-06 → 2026-05-06.

Figure 11: CWA buoy Hs vs WAVERYS analysis-forecast Hs, 30-day window 2026-04-06 → 2026-05-06, 3-hourly aligned. Top panel: Hsinchu 46757B (nearest CWA wave buoy to North site, ~36 km offshore). Bottom panel: Qimei C6W10 (nearest CWA wave buoy to both South ~22 km and Middle ~96 km). Per-panel stats annotated; "nearest study site" in panel title flags which study site(s) the buoy is the nearest CWA wave buoy for. The Middle site's 96 km distance to Qimei means the Qimei result is used as a supporting check for Middle, not a site-direct measurement — see §8.3 item 12 caveat scope.

7.3 Interpretation summary

The §7.1 seasonal-cycle agreement at all three sites (mean-Hs r $\geq$ 0.97 at N + M, r = 0.77 at S) **supports the seasonal-cycle aspect** of the §3 – §6 WAVERYS-based climatology characterisation. This does **not** extend to validating absolute Hs magnitudes — the ~0.25 m systematic positive WAVERYS bias is not small in absolute terms — nor does it extend to extreme-value validation. The bias is consistent across the three sites and is methodologically attributable to either a NE-monsoon-window difference (2019-2023 vs 2008-2017) or the known WAVERYS / MFWAM mild positive bias under moderate-to-strong wind-sea regimes. The §7.2 buoy-level model agreement at Hsinchu and Qimei (RMSE $\approx$ 0.23-0.25 m, r $\approx$ 0.85-0.88) is supporting evidence for model-family reasonableness during a calm-regime 30-day window — not for design-level or extreme-event validation — at North and South; at Middle, where no close buoy exists, the Qimei result is used only as a weaker supporting check, not as a site-direct measurement. Neither §7.1 nor §7.2 constitutes a formal design-load validation; for absolute-extreme statistics and at-site historical buoy validation, formal extreme-value analysis with purchased CWA historical buoy time series is required and is out of scope of this desktop-study report.

8. Limitations and caveats (consolidated)

Every number in §3 – §7 sits inside a set of limits — what the source data can and cannot capture, what the analysis methodology can and cannot resolve, what the 5-year window can and cannot tell you, and what an operability tier means in practice. The 15 caveats below state those limits up front so each headline number can be read with the right level of confidence. They are organised by theme rather than as a flat list, and reflect methodological discipline at the screening-study level rather than a list of report weaknesses.

8.1 Source-data accuracy

1. **Reanalysis under-representation of compact intense TC peaks.** The 20–40% under-estimation range is well-documented for reanalysis tropical-cyclone intensity (Hodges et al. 2017; Schenkel & Hart 2012). ERA5 (Hersbach et al. 2020) provides higher native resolution and 4D-Var assimilation than ERA-Interim / JRA-55, but neither eliminates the bias for small-radius intense cyclones. The WAVERYS multiyear reanalysis used here additionally assimilates altimeter SWH (and post-2017 Sentinel-1 SAR directional spectra), which partially mitigates the wind-driven Hs bias, but altimeter overpasses are sparse at eyewall spatial scales — so per-site Hs values during compact intense TC passages should be treated as **indicative, not design-level**. Absolute-extreme typhoon analysis requires bias correction or a different data source, and is out of scope for this desktop-study report.
2. **ERA5 100 m wind is a model diagnostic, not assimilated.** Bias risk in stable boundary layers; project-specific hub-height climatology benefits from validation against a met mast or higher-resolution mesoscale model at each of the three sites.
3. **ERA5 0.25° smooths the NE-monsoon low-level jet** through the Strait. Local channelling not fully resolved; mean wind speed in the 10–20 m/s range is slightly understated, and the effect applies to all three sites with the strongest impact expected at the central Strait where the channel funnel is most pronounced (consistent with the §3.1 Middle p95 ranking).
4. **WAVERYS partition Hs can mildly exceed total Hs** (~6% in ≈0.002% of cells) due to known WAM-family/WW3 spectral bin-assignment behaviour. Not a data error; uses of partition VHM0 values exceeding total VHM0 should fall back to total VHM0 at those timestamps.
5. **ERA5 SST land contamination** at coastal cells of the extraction extent. None of the three site coordinates lies in a cell containing land, and the bilinear stencils at each site fall on open Strait cells well separated from both the Fujian and Taiwan coasts (the nearest bilinear-stencil corner cell at any site is $\geq$ 30 km from the nearest mainland or main-island coast). Spatial *means* computed over the full 22–26°N / 117–122°E extraction extent, however, contain coastal cells along both the Fujian and Taiwan coastlines, and must apply a sea-only mask. Site time series in this report use bilinear-only and do not propagate land contamination at any of the three sites.

8.2 Spatial and temporal resolution

6. **Three off-grid sites; bilinear at each.** The selection-point methodology (§2.2) is exercised three independent times against the same ERA5 0.25° × 0.25° and WAVERYS 0.2° × 0.2° grids. North (25.00°N, 120.44°E) is off-grid in both dimensions for both products. Middle (24.05°N, 119.80°E) —

on-grid in longitude for WAVERYS (which uses 0.2° native), off-grid in both dimensions for ERA5. South (23.00°N, 119.57°E) is off-grid in both dimensions for both products.

7. **Bilinear vs nearest-neighbour sensitivity**. Verified at the Middle coordinate in prior characterisation work (negligible for mean / median / p95; a few-percent shift on absolute extremes). The same regime is expected to apply at North and South given the analogous coastal extraction-extent geometry; explicit per-site sensitivity bars are deferred to a later round and are not expected to alter the headline rankings.
8. **IBTrACS catalogue completeness — extraction methodology**. The §6.1 catalogue is built by reading the full IBTrACS v4r01 archive directly and applying storm-level filters: (a) Western-Pacific basin classification at the first track point, (b) season 2019–2023, (c) lifetime peak USA 1-min sustained wind $\geq$ 34 kt, (d) any track point within 200 km of any of the three sites. This avoids any extent-driven completeness gap at the North and South 200 km filter circles. Residual completeness boundaries that the analysis cannot detect: (i) storms classified in a non-WP basin at first track point that then enter the study area (negligible risk for this latitude band given Western-Pacific track climatology, but not directly verified), (ii) genuine IBTrACS-archive limitations for any unrecorded systems — assumed negligible at TS+ intensity in the WP basin where multi-agency reporting is comprehensive.
9. **3-hourly joint frame alignment** between ERA5 hourly and WAVERYS 3-hourly waves: direct downsampling at the WAVERYS timestamps (§2.3). Brief sub-3-hour Hs spikes between WAVERYS samples cannot be captured in the joint frame by construction; this is intrinsic to the WAVERYS sampling cadence and applies equally to all three sites. The §5.2 persistence statistics (median operable-window duration on the order of 36–39 hours at Tier B) are well above the 3-hour quantisation floor and are not materially affected.
10. **5-yr window stability for p95 / p99**. The per-site annual percentile statistics in §3.1 (wind10 p95/p99) and §4.1 (Hs p95/p99) are based on n = 43,824 hourly samples (wind) and n = 14,608 3-hourly samples (Hs) per site. The 5-yr window resolves the p95 with high precision and the p99 with moderate sampling noise; the p99 site ordering across the three sites is stable. The ~5–10% interval often quoted for empirical p99 is an independent-sample heuristic; in this record the storm-event clustering (Hs is strongly autocorrelated within multi-day monsoon and typhoon events) reduces the effective independent sample count materially below the raw n, so the true p99 uncertainty band is wider than the naive 5–10% estimate suggests. Absolute 5-yr maxima (Hs max at South, 7.65 m; wind10 max at all sites) are single-event statistics and inherit substantially larger uncertainty — the rank ordering at the absolute max is sample-dependent.

8.3 Catalogue and cross-validation scope

11. **IBTrACS catalogue filters and sample-size asymmetry**. The §6.1 catalogue is restricted to (a) tracks passing within 200 km of any of the three sites and (b) systems whose lifetime peak wind reached at least Tropical Storm intensity ($\geq$ 34 kt). Per-site sample sizes are asymmetric: North n = 3, Middle n = 6, South n = 8. Closest-pass *minimum* comparisons across the three sites are sensitive to this asymmetric sample size (see §6.1 prose and §6.2 table footnote). Tropical-Depression-only systems are excluded; for low-energy-event screening this filter should be relaxed.
12. **Cross-validation scope at this desktop-study tier**. §7.1 (CWA WW3 10-yr vs WAVERYS 5-yr

seasonal-cycle check at three sites) and §7.2 (CWA buoy vs WAVERYS-NRT 30-day Hs tracking at the two nearest buoys, Hsinchu and Qimei) are the cross-validation evidence carried in this report. Three structural limitations: (a) §7.1 compares **non-overlapping decadal windows** (2008-2017 CWA vs 2019-2023 WAVERYS), so any 0.1-0.3 m systematic bias may partly reflect inter-decadal forcing variability rather than model-vs-model offset; (b) §7.2 uses the WAVERYS **analysis-forecast** variant during a recent 30-day rolling window, not the multi-year reanalysis used in §3 – §6 — bias magnitudes reflect the overall reasonableness of the WAVERYS / MFWAM model series, not the specific bias of the reanalysis variant; (c) the Middle site has no CWA wave buoy closer than ~96 km (see §7.2 site-distance table) and the **Penghu Islands sit between Qimei buoy (south of Penghu) and Middle (central Strait, north of Penghu)** as a partial topographic / bathymetric obstacle to wave propagation — so the §7.2 buoy result at Middle is used as a supporting check (with strength depending on Qimei's 96 km distance and the Penghu shadow) rather than site-direct validation, and the 96 km straight-line distance itself understates the functional oceanographic separation; (d) the §7.2 30-day window 2026-04-06 → 2026-05-06 falls in the **spring-transition season** (post-NE-monsoon, pre-SW-monsoon) with Hs predominantly low-to-moderate; the §7.2 RMSE / r values therefore characterise WAVERYS-family skill under a calm regime, not under the NE-monsoon winter regime that drives the §3 – §6 climatology tail and the §5.1 operability fractions. At-site historical CWA buoy time series (CWA's 申購 purchase tier) and formal extreme-value analysis are out of scope of this desktop-study report.

8.4 Operability-framework modelling choices

13. **Operability-tier wind threshold is the mean wind speed**, not the gust speed. ERA5 marine 3-second gust at these three sites under **routine NE-monsoon conditions** is typically 1.3–1.5× the mean. Under **typhoon eyewall convection**, marine surface gust factors can reach 1.5–1.7× or higher and require a separate assessment. Customer-facing operability should be re-tabulated against the relevant gust threshold for the actual vessel / crane envelope; the headline Tier-A/B/C fractions in §5.1 are mean-wind based.
14. **Marginal-distribution stats cannot be linearly combined into joint operability**. At all three sites Hs and wind10 are strongly correlated during the NE-monsoon season (storm-time co-occurrence) and more nearly independent during the SW-monsoon. The Tier A/B/C operability fractions are joint computations from the joint frame for the specific thresholds reported; they cannot be reconstructed from the §3 / §4 marginal distributions for thresholds not specifically computed.
15. **Long-period swell is not used as an operability criterion** in §5. The §5.1 tiers use only Hs and wind10; the §4.4 long-period (Tp $\geq$ 10 s) sample fractions (N 3.5% / M 2.1% / S 2.9%), the §4.5 partition decomposition (South SW1 47.9% of energy), and the §4.6 VTPK switch-in-mixed-seas caveat are not folded into the tier definitions. For motion-sensitive operations (crane envelope, CTV transfers, floating-asset response) a swell-period-aware operability framework — and a customer-specific tier specification using partition mean periods (VTM01_SW1) or motion-relevant Te / Tm-1,0 — is the cleaner descriptor. The partition variables are present in the per-site WAVERYS Parquets for that customer-specific build-out.

This level of explicit limitation is part of the desktop-study posture: clear about what the analysis can and cannot bear at Level 1.

9. Data sources, attribution, and licensing

ERA5 reanalysis: Generated using Copernicus Climate Change Service Information [2026]. Licence: CC-BY 4.0. Source: Climate Data Store (cds.climate.copernicus.eu). Hourly: DOI 10.24381/cds.adbb2d47. Monthly: DOI 10.24381/cds.f17050d7.

Copernicus Marine WAVERYS (GLOBAL_MULTIYEAR_WAV_001_032 v202411): Generated using E.U. Copernicus Marine Service Information; DOI 10.48670/moi-00022. Licence: CMEMS Licence.

IBTrACS (International Best Track Archive for Climate Stewardship), v4r01: NOAA NCEI public-domain global tropical-cyclone best-track archive (Knapp et al. 2010, DOI 10.1175/2009BAMS2755.1). Used in §6.1 for the per-site typhoon exposure catalogue, 2019–2023 window, Western-North-Pacific basin. The archive is in the public domain; attribution is courteous but not mandated.

CWA OpenData `C-B0086-001` (台灣海域波候統計, 2008–2017 monthly Hs climatology on 0.25° grid, modelled with WaveWatch III by 中央氣象署 CWB / CWA): used in §7.1 as the independent decadal seasonal-cycle reference. Open licence: 政府資料開放授權條款第 1 版 (Open Government Data License v1.0). Source: opendata.cwa.gov.tw.

CWA OpenData `O-B0075-002` (海象觀測資料-海面氣象站浮標即時, rolling 30-day window): used in §7.2 for buoy / WAVERYS-NRT cross-check at Hsinchu (46757B) and Qimei (C6W10). Same Open licence as above. Source: opendata.cwa.gov.tw.

CMEMS WAVERYS analysis-forecast (`cmems_mod_glo_wav_anfc_0.083deg_PT3H-i`): used in §7.2 (NRT variant) as the WAVERYS-family product for the 30-day buoy / model comparison window. Generated using E.U. Copernicus Marine Service Information; DOI 10.48670/moi-00017. Licence: CMEMS Licence. This variant differs from the GLOBAL_MULTIYEAR_WAV_001_032 reanalysis used in §3 – §6 in its assimilation stream and forcing window (see §7.2 note).

Coastlines (Figure 1 site map and Figure 9 typhoon tracks): Natural Earth via cartopy.

Cited literature

- Hersbach, H., et al. (2020). The ERA5 global reanalysis. *Quarterly Journal of the Royal Meteorological Society*, 146(730), 1999-2049. DOI 10.1002/qj.3803.
- Hodges, K., Cobb, A., & Vidale, P. L. (2017). How well are tropical cyclones represented in reanalysis datasets? *Journal of Climate*, 30(14), 5243-5264. DOI 10.1175/JCLI-D-16-0557.1.
- Schenkel, B. A., & Hart, R. E. (2012). An examination of tropical cyclone position, intensity, and intensity life cycle within atmospheric reanalysis datasets. *Journal of Climate*, 25(10), 3453-3475. DOI 10.1175/2011JCLI4208.1.
- Knapp, K. R., Kruk, M. C., Levinson, D. H., Diamond, H. J., & Neumann, C. J. (2010). The International Best Track Archive for Climate Stewardship (IBTrACS): Unifying tropical cyclone data. *Bulletin of the American Meteorological Society*, 91(3), 363-376. DOI 10.1175/2009BAMS2755.1.
- Stopa, J. E. (2018). Wind forcing calibration and wave hindcast comparison using multiple reanalysis and merged satellite wind data. *Ocean Modelling*, 127, 55-69. DOI 10.1016/j.ocemod.2018.04.008.

- Copernicus Marine Service. Quality Information Document (QUID) for the WAVERYS Global Wave Reanalysis product (`GLOBAL_MULTIYEAR_WAV_001_032`). Available via the Copernicus Marine product catalogue.

Per-dataset access dates, source file checksums, and the version-control commit identifiers for the download and processing workflows are recorded in the case manifest, available on request.

---

10. Reproducibility

Every numerical result and figure in this report regenerates from a versioned analysis pipeline. The pipeline comprises:

1. **Data ingestion**: source data is fetched from each provider (ERA5 from CDS, WAVERYS from Copernicus Marine; the 22–26°N × 117–122°E extraction extent covers all three sites). Each source file's SHA-256 checksum is recorded in the case manifest.
2. **Site extraction**: bilinear interpolation at the selection point, with cross-variable time-index validation guarding against silent NaN-padding.
3. **Statistical analysis**: monthly and annual climatology, joint-threshold operability tiers, and operability-window persistence (run-length distribution).
4. **Cross-validation**: alternative-source per-site spot checks against open-licence products — CWA WW3 10-yr hindcast (`C-B0086-001`) for seasonal-cycle consistency, and CWA buoy real-time data (`O-B0075-002`) + WAVERYS analysis-forecast for synoptic Hs tracking at the two nearest buoys. See Section 7.
5. **Visualisation**: every figure is produced through a reproducible plotting workflow; the figures are listed in Annex A.
6. **Quality assurance**: validates downloaded data against expected dimensions, bounds, and manifest checksums.

Production workflow. This report is produced through an AI-assisted workflow. Data ingestion, analysis design, figure generation, and report drafting all run within the reproducible pipeline above; methodology assumptions, interpretive claims, and limitations are made explicit inline. The workflow emphasises source-traceability and reproducibility — every figure caption, table value, and section finding traces to a specific data product and processing step. (Scope limits that apply to any early-stage desktop study — independent of production method — are stated in the Disclaimer and Section 8.)

Access. The codebase, manifest, and reproduction instructions are available on request — `contact@pfts.com.tw`.

Annex A — Figures index

Table 17: Figures index.

Figure	Section	Description
1	1	Three Taiwan Strait sites used in this study — spatial layout map
2	3.2	Monthly mean 10 m wind speed at three Taiwan Strait sites — three-site overlay
3	3.3	10 m wind direction roses at three Taiwan Strait sites — three-panel comparison
4	4.2	Monthly mean Hs at three Taiwan Strait sites — three-site overlay
5	4.3	Three-site paired wind + wave roses with per-site directional offset $\Delta\theta$
6	4.4	Joint distribution of Hs and Tp at three Taiwan Strait sites — hexbin density
7	4.5	Primary-swell (SW1) direction roses at three Taiwan Strait sites — partition decomposition
8	5.2	Operability persistence survival curves — three-site three-tier panel layout
9	6.1	Typhoon tracks within 200 km of any of the three study sites (IBTrACS 2019–2023) — regional map
10	7.1	CWA WW3 10-yr vs WAVERYS 5-yr monthly mean Hs cross-check at three sites
11	7.2	CWA buoy vs WAVERYS-NRT 30-day Hs tracking at Hsinchu and Qimei buoys

All figures are produced by reproducible analysis workflows referenced in the case manifest (available on request).

Annex B — Stats tables index

Table 18: Stats tables index.

#	Table
B-1	Per-site monthly mean / percentile wind10 stats — extended detail behind §3.1
B-2	Per-site monthly mean / percentile Hs / Tp stats — extended detail behind §4.1
B-3	Per-site joint-frame operability fractions, all tiers × monthly + annual — extended detail behind §5.1
B-4	Per-site Tier-A / B / C operable + downtime run-length distributions (annual) — extended detail behind §5.2
B-5	Per-site IBTrACS typhoon catalogue (storm × site, 2019–2023, TS+ within 200 km) — extended detail behind §6.1
B-6	Cross-segment critical-parameter differential summary (long form: metric × site rows with rank and spread) — extended detail behind §6.2
B-7	Per-site CWA WW3 vs WAVERYS monthly Hs cross-check table (mean / median / max + bias / RMSE / r per month per site) — extended detail behind §7.1

#	Table
B-8	Per-site CWA buoy vs WAVERYS-NRT 30-day Hs cross-check table (per-buoy n / means / bias / RMSE / r + per-site nearest-buoy distances) — extended detail behind §7.2